PHYSICAL REVIEW D VOLUME 11, NUMBER 10 15 MAY 1975

Solid neutron matter*

M. T. Takemori and R. A. Guyer
Department of Physics and Astronomy, University of Massachusetts, Amherst, Massachusetts 01002
(Received 18 July 1974; revised manuscript received 14 January 1975)

The ground state of solid neutron matter is investigated using the t-matrix formalism developed for the quantum crystal problem. Studies of neutrons interacting through the repulsive part of the Reid $^1S_0$ interaction, the Reid $^1S_0$ interaction, and the full Reid potentials are made in the Hartree, Hartree t-matrix, Hartree-Fock, and Hartree-Fock t-matrix approximations. The results of the studies of the two model problems, the repulsive part of the $^1S_0$ interaction and the $^1S_0$ interaction, are exhibited and discussed in detail. These model problems provide a test of the computational procedures employed in using the quantum crystal formalism on the neutron matter problem. The result of the study of neutrons interacting through the Reid soft-core potentials is described. We find no evidence in the study of either of the model problems for the presence of a solid ground state. Further, we find no evidence in the study of neutrons interacting through the full set of Reid soft-core potentials for the presence of a solid ground state.

I. INTRODUCTION

The possibility of a phase transition of neutron matter from a liquid phase to a solid phase has been suggested by a number of recent theoretical investigations[1] and astrophysical observations.[2] The solid-neutron-matter problem is the theoretical problem of learning whether a liquid-solid phase transition exists, and if it does, at what density or pressure it exists and the properties of the resulting solid state. This problem is an integral part of the overall problem of the equation of state of dense matter.

There have been a number of recent investigations of the solid-neutron-matter problem; they are listed here along with useful information about each calculation.[3-7]

1. Anderson and Palmer. The neutron-neutron interaction is scaled to a core-shifted Lennard-Jones 6-12 potential. The neutron matter problem is then mapped onto the $T=0$ rare-gas problem using the de Boer theory of corresponding states. A liquid-to-solid phase transition is found at a density of 3.3×10^{14} g/cm^3 (see also the work of Clark and Chao[3]).

2. Schiff. The repulsive part of the neutron-neutron interaction is replaced by a hard sphere. The resulting unperturbed system, the hard-sphere—Bose system, is corrected for the weak attractive interaction and statistics. A liquid-to-solid transition is found at 2.9×10^{15} g/cm^3.

Both the calculation of Anderson and Palmer and that of Schiff map the neutron matter problem onto another problem that is known to have a liquid-solid transition. Thus the crucial question in attempting to assess the validity of the conclusions reached in these calculations is whether the mapping employed is valid for neutron matter.

3. Pandharipande. A modified version of the Reid interaction is employed. Pandharipande uses a constrained variation of the energy approximated by the one- and two-body terms in the Van Kampen cluster expansion to examine both the liquid and solid states. No liquid-to-solid phase transition is found up to 5.8×10^{15} g/cm^3.

4. Nosanow and Parish. A simplified version of the Reid interaction is employed. A parametrized Jastrow factor is used in a variational calculation of the energy by a Monte Carlo integration scheme. Both the liquid and solid phases are studied. A liquid-to-solid transition is found at 4.2×10^{14} g/cm^3.

5. Østgaard. A simplified state-independent potential is employed. The computational scheme is the variational form of the t-matrix formalism developed for the quantum crystals. No evidence for a liquid-solid phase transition is found up to 2.0×10^{15} g/cm^3.

6. Canuto and Chitre. The full set of state-dependent Reid soft-core potentials is employed. The computational scheme is the self-consistent form of the t-matrix formalism developed for the quantum crystals. A neutron solid state was found for the system at all relevant densities.[8] Comparison of the liquid energy (from Pandharipande) and solid energy led to a liquid-solid phase transition at 1.6×10^{15} g/cm^3.

The calculation of Canuto and Chitre is by far the most ambitious of the microscopic calculations on the solid-neutron-matter problem. It

employs the best neutron-neutron interaction available (without approximation) and a computational scheme that has been well tested against the laboratory quantum crystals.

It is apparent from the disparity of the results of these calculations that the solid-neutron-matter problem is still unsolved. Comparison between the various calculations is made difficult by the wide variety of nuclear interactions and computational methods utilized. In order to test the various computational methods employed in doing the solid-neutron-matter problem, several research groups agreed to use their computational methods on a "homework" problem and to compare the results. The homework problem consisted of using the repulsive part of the Reid $^1S_0$ potential with no symmetry effects. Canuto, Lodenquai, and Chitre[9] obtained values of E/N (energy/particle) for the homework solid state (using the computational methods of Canuto and Chitre) which are in reasonable agreement with the homework results of Chakravarty, Miller, and Woo.[10] Both of these results for E/N differed from those of Pandharipande. Results for the homework problem were not obtained from Nosanow and Parish. From this test it was concluded that the computational method of Canuto and Chitre was more reliable than that of Pandharipande.[10]

Although the E/N results obtained by Canuto, Lodenquai, and Chitre and by Chakravarty, Miller, and Woo for the homework problem are in reasonable agreement, the "solid" states obtained in each of these calculations are very different. Chakravarty, Miller, and Woo obtain a "solid" state with values of α^2 (α^2 is a measure of the size of the wave function of a particle on a lattice site) between 0.4 and 1.0. This range of α^2 corresponds to single-particle wave functions that span 10—20 lattice sites. The "solid" state of Chakravarty, Miller, and Woo is thus best regarded as an alternate liquid state. Canuto, Lodenquai, and Chitre find substantially more compact single-particle wave functions than Chakravarty, Miller, and Woo. Nonetheless, their wave functions describe a solid with particles substantially less well localized on their lattice sites than any known solid system. We believe the agreement of the values of E/N calculated by Canuto, Lodenquai, and Chitre and Chakravarty, Miller, and Woo is at best fortuitous. Unfortunately, this does not reinstate the solid-neutron-matter calculations of Pandharipande as Woo and Shen[11] have faulted them on other grounds.

The contradictory results obtained in the theoretical studies of the solid-neutron-matter problem thus remain unresolved. Further, there is no definite experimental evidence for the existence of solid neutron matter. Thus it is necessary that in presenting the results of a calculation on the solid-neutron-matter problem, one makes a serious attempt to demonstrate the credibility of the calculation. In this context we wish to emphasize that theoretical treatment of the laboratory quantum crystals require formalisms of marked complexity compared to those formalisms which are used to treat the classical crystals. Nonetheless, the laboratory quantum crystals are known to have properties that are, at most, the extreme limit of similar properties for the classical crystals. Further, the laboratory quantum crystals are described by wave functions that are understandably related to their known properties.[12] Plausible expectations for the properties of the laboratory quantum crystals are borne out in practice. We have the same expectations for the neutron quantum crystal and we employ these expectations in the assessment of the outcome of our calculations.

We have undertaken a careful and systematic study of the ground-state properties of solid neutron matter. The most reliable nuclear potentials, the Reid potentials,[13] are state-dependent and extremely complex, thus precluding a simple understanding of the basic physics of the system. Thus we have chosen to examine two spin- and state-independent model potentials as well as the full set of Reid potentials.[14] The model potentials we have examined are the "homework" potential and the Reid $^1S_0$ soft-core potential. The nuclear potentials are not excessively attractive so that their repulsive core is the most important feature for bringing about solidification. The purely repulsive "homework" potential, our first model problem, should thus crudely approximate the behavior of the neutron system in the limit of no attractive interaction. The second model problem, the $^1S_0$ potential, uses the most attractive Reid potential and as such should thus crudely approximate the behavior of the neutron system in the opposite limit. We have chosen to study these model potentials under a sequence of increasingly sophisticated approximations, the Hartree, Hartree-Fock, Hartree t-matrix, and the Hartree-Fock t-matrix approximations. Each of these is a two-body approximation to the energy of the system. The model problems employ state-independent neutron-neutron interactions. They can therefore be solved in an approximation that localizes a particular particle on a particular lattice site or that permits particles to exchange with one another and be localized on two lattice sites. The first approximation, a particle localized on a particular lattice site, is called the

Hartree approximation since particle exchange is not permitted. When a pair of particles, each localized near its own lattice site, is correlated at small r by the interaction between them, we refer to this as the Hartree t-matrix approximation. The second approximation, particles localized on a pair of lattice sites, is called the Hartree-Fock approximation since particle exchange is permitted. When the pair of particles so localized is correlated at small r by the interaction we refer to this as the Hartree-Fock t-matrix approximation. When a state-dependent neutron-neutron interaction is used, partial-wave decomposition of the pair wave function is required. The resulting partial-wave components of the wave function have symmetries that are not preserved in a Hartree description of the system that localizes a particular particle on a particular site. Thus the full solid-neutron-matter problem can only be done in the Hartree-Fock approximation. When a state-independent neutron-neutron interaction is used, partial-wave decomposition of the pair wave function is not required. Thus the model problems can be solved in all four approximations. We can use the relatively straightforward Hartree and Hartree t-matrix solutions of the model problems to test the adequacy of the much more difficult Hartree-Fock and Hartree-Fock t-matrix solutions. It is this last approximation, the Hartree-Fock t-matrix approximation, that we have used on the full solid-neutron-matter problem. The sequence of approximations we have studied permits us to exhibit the evolution of the method of calculation from the Hartree to the Hartree-Fock t-matrix approximation, as applied to the model potentials. Further, this sequence of approximations provides tractable results on which we can apply physical tests and on which we can sharpen our intuition about the behavior of the system. It is through this systematic investigation of the model potentials that we hope to demonstrate the validity of our results for the full neutron solid problem.

The outline of the rest of the paper is as follows: In Sec. II we exhibit the equations employed in the four approximations we use. In Sec. III we describe the results of the application of each of these approximations to the homework problem and the problem generated by the Reid $^1S_0$ soft-core potential. These results are discussed in detail. In Sec. IV we state our expectations for the results for the full solid-neutron-matter problem and we exhibit the results of a Hartree-Fock t-matrix calculation on this problem. We complete Sec. IV with critical comments on a number of the existing solid-neutron-matter calculations using the understanding we have gleaned from our model problems as a guide. We summarize our results in Sec. V. A number of useful details are discussed in Appendixes A, B, C, and D.

II. FORMALISM

In this section we outline the formalism we have employed in doing our calculations on solid neutron matter. We discuss the results of the application of this formalism in Sec. III below. We have worked on the solid-neutron-matter problem using a number of approximations with varying degrees of sophistication. In order to make comments on the results of each of our calculations as specific as possible we include in this section a systematic description of the set of computational equations employed in each approximation.

The system to be described is a lattice of N neutrons occupying volume V and interacting with one another through the Reid soft-core potentials.[13] The Hamiltonian describing this system is

$$\mathcal{H} = \sum_i T(i) + \tfrac{1}{2} \sum_{ij}{}' v(ij), \tag{1}$$

where $T(i)$ is the kinetic energy operator and $v(ij)$ is the interaction between a pair of neutrons. [The prime on the summation indicates that $j = i$ is excluded in the double sum; we later use $j \neq (i)$ to mean sum on j except for $j = i$.] The pair interaction in Eq. (1) is given by the Reid soft-core potentials which have matrix elements

$$v_{LL'}^{JS}(r) = \langle r; JM_J, LS | v | r; J'M_{J'}, L'S' \rangle \times \delta_{JJ'} \delta_{M_J M_{J'}} \delta_{SS'} \delta_{L,(L' \text{ or } L' \pm 2)}, \tag{2}$$

where $\vec{J}$ and $\vec{S}$ are the total angular momentum and total spin angular momentum of a pair of neutrons. These potentials cause pairs of particles in a particular $\vec{J}$, $\vec{S}$ state to interact with one another in a way that at most couples their relative orbital angular momentum. Because of the state-dependent nature of the Reid soft-core potentials, the wave function describing a pair of particles must be decomposed into partial waves which exhibit the appropriate spatial symmetry to properly antisymmetrize the total pair wave function. When employing such properly antisymmetrized pair wave functions, it is necessary to describe the pair of particles by a Hamiltonian consistent with their symmetry, i.e., to employ a parity-conserving Hamiltonian.

To reveal important features of a complicated physical system, it is often useful to do approximate calculations with a simplified system. The full Reid soft-core potentials are extremely complex and thus a complete understanding of the results of a problem involving them is very dif-

ficult. For this reason, we have chosen to initially examine two model potentials which are much simpler than the Reid soft-core potentials. We expect that these model potentials will approximately describe the behavior of the full Reid soft-core potentials:

(1) the repulsive interaction,

$$v_R(r) = 6484.2\,\frac{e^{-7x}}{x}\,, \tag{3}$$

(2) the $^1S_0$ interaction,

$$v_{^1S_0}(r) = -10.463\,\frac{e^{-x}}{x} - 1650.6\,\frac{e^{-4x}}{x} + 6484.2\,\frac{e^{-7x}}{x}, \tag{4}$$

where $x = \mu r$ and $\mu = 0.7\ \mathrm{F}^{-1}$. The repulsive interaction $v_R(r)$ is the repulsive part of the $^1S_0$ Reid soft-core potential and $v_{^1S_0}(r)$ is the full $^1S_0$ Reid soft-core potential. The repulsive interaction $v_R(r)$ has been previously used to define the "homework" potential. The potentials v_R and $v_{^1S_0}$ are state-independent, i.e., the same for all L. These model potentials can thus be studied in some approximations without recourse to the complicated partial-wave equations necessary when employing the full state-dependent Reid soft-core potentials. However, in the Hartree-Fock t-matrix approximation for the model potentials we use the partial-wave equations.

The model neutron solid problems defined by Eqs. (1), (3), and (4) are solved in four approximations: Hartree, Hartree-Fock, Hartree t matrix, and Hartree-Fock t matrix. The theory of the t-matrix approach to these problems is extensively discussed in many recent works.[15] Here we briefly review the most important equations.

The ground-state energy per particle of the system described by $\mathcal{H}$ in Eq. (1) is given to second order in Rayleigh-Schrödinger perturbation theory as

$$\frac{E}{N} = \frac{3}{4}\,\frac{\hbar^2}{m}\,\alpha^2 + \tfrac{1}{2}\,\overline{U}\,, \tag{5}$$

where $\frac{3}{4}(\hbar^2/m)\alpha^2$ is the kinetic energy per particle and $\frac{1}{2}\overline{U}$ is the average potential energy per particle. The unperturbed system is described in terms of self-consistent single-particle wave functions

$$\phi_i(i) = \left(\frac{\alpha^2}{\pi}\right)^{3/4} \exp\left[-\frac{\alpha^2}{2}\,(\vec{\mathbf{x}}_i - \vec{\mathbf{R}}_i)^2\right], \tag{6}$$

which localize particle i near lattice site $\vec{\mathbf{R}}_i$ and are normalized to 1. The parameter α^2, which describes the width of the single-particle wave function, is determined from the self-consistency condition

$$\alpha^2 = \frac{4}{3}\,\frac{m}{\hbar^2}\,(\overline{U} - U_0)\,, \tag{7}$$

where U_0 is the depth of the single-particle potential well which shapes the single-particle wave function. The potential energy quantities $\overline{U}$ and U_0 are computed as functions of α^2 using equations specific to the particular approximation being employed. When α^2 is regenerated through the self-consistency equation, Eq. (7), this value of α^2 is labeled $\alpha_{SC}{}^2$ and is used to compute the ground-state energy per particle of the system in Eq. (5).

1. Hartree approximations. The Hartree approximations employ localized wave functions with no symmetrization. The state-independent model potentials can be analyzed in the Hartree approximation whereas the state-dependent Reid soft-core potentials cannot be correctly treated in this unsymmetrized manner. In the Hartree approximations $\overline{U}$ and U_0 are given by

$$\overline{U} = \sum_{j\neq(i)} \frac{\int d\vec{\mathbf{x}}_i \int d\vec{\mathbf{x}}_j \phi_i(i)^* \phi_j(j)^* v(ij)\psi(ij)}{\int d\vec{\mathbf{x}}_i \int d\vec{\mathbf{x}}_j\, \phi_i(i)^* \phi_j(j)^*\, \psi(ij)} \tag{8}$$

and

$$U_0 = \left(\frac{\alpha^2}{\pi}\right)^{-3/2} \times \sum_{j\neq(i)} \frac{\int d\vec{\mathbf{x}}_i \int d\vec{\mathbf{x}}_j\, \phi_i(i)^* \phi_j(j)^* v(ij)\delta^3(\vec{\mathbf{x}}_i - \vec{\mathbf{R}}_i)\psi(ij)}{\int d\vec{\mathbf{x}}_i \int d\vec{\mathbf{x}}_j\, \phi_i(i)^* \phi_j(j)^* \psi(ij)}\,, \tag{9}$$

where $\phi_i(i)$ is the single-particle wave function of Eq. (6) and $\psi(ij)$ is the correlated pair wave function obtained by solving the "Hartree" Bethe-Goldstone equation

$$[T(i) + T(j) + U_i(i) + U_j(j) + v(ij)]\,\psi(ij) = \epsilon_{ij}\psi(ij), \tag{10}$$

where

$$U_i(i) = U_0 + \frac{1}{2}\,\frac{\hbar^2}{m}\,\alpha^4(\vec{\mathbf{x}}_i - \vec{\mathbf{R}}_i)^2\,. \tag{11}$$

When $\psi(ij)$ is written in the Jastrow form

$$\psi(ij) = g(\vec{\mathbf{r}})\phi_i(i)\phi_j(j)\,, \tag{12}$$

$g(\vec{\mathbf{r}})$ is known as the pair correlation function (where $\vec{\mathbf{r}} = \vec{\mathbf{x}}_i - \vec{\mathbf{x}}_j$). We treat $g(\vec{\mathbf{r}})$ in two ways: (a) we solve Eq. (10) for $\psi(ij)$ or $g(r)$ in the one-dimensional approximation of Guyer and Sarkissian; (b) we ignore Eq. (10) and take $g(r)$ to be a simple cutoff:

$$g(r) = \theta(r - r_0) = \begin{cases} 1, & r \geq r_0 \\ 0, & r < r_0\,. \end{cases} \tag{13}$$

We choose values of r_0 ranging from $r_0 = 0$ (uncorrelated) to $r_0 = 1.0$ fermi. The choice $r_0 = 0$ yields $g(r) = 1$, $\psi(ij) = \phi_i(i)\phi_j(j)$. The problem that results in this limit we refer to as the "Hartree problem." When $g(r)$ is given by Eq. (13) for $r_0 \neq 0$ we refer to the problem that results as the "correlated Hartree problem." When $g(r)$ is given by solving Eq. (10) we refer to this problem as the "Hartree t-matrix problem."

2. Hartree-Fock approximations. In a Hartree-Fock description of the solid problem each of the pair of particles spends some time at both of the lattice sites associated with the pair. The wave function for a pair of particles must be properly antisymmetrized and the pair Hamiltonian which describes the motion of a pair of particles must be properly symmetrized (parity conserving). Furthermore, a particular spin arrangement must be defined for the solid. In the Hartree-Fock approximations $\overline{U}$ is given by

$$\overline{U} = \sum_{j \neq (i)} [\overline{U}_{\uparrow\uparrow}(ij)\delta_{\uparrow\uparrow, ij} + \overline{U}_{\uparrow\downarrow}(ij)\delta_{\uparrow\downarrow, ij}] . \tag{14}$$

As the particles are indistinguishable i and j refer to lattice sites rather than particles. We have

$$\delta_{\uparrow\downarrow, ij} = \begin{cases} 1 & \text{if the spin at site } i \text{ is } \uparrow \\ & \text{and the spin at site } j \text{ is } \downarrow, \\ 0 & \text{otherwise.} \end{cases} \tag{15}$$

The potential energies $\overline{U}_{\uparrow\uparrow}(ij)$ and $\overline{U}_{\uparrow\downarrow}(ij)$ are given by

$$\overline{U}_{\uparrow\uparrow}(ij) = \frac{\int d\vec{x}_i \int d\vec{x}_j \phi^-(ij)^* v(ij) \psi^-(ij)}{\int d\vec{x}_i \int d\vec{x}_j \, \phi^-(ij)^* \psi^-(ij)} \tag{16}$$

and

$$\overline{U}_{\uparrow\downarrow}(ij) = \frac{\int d\vec{x}_i \int d\vec{x}_j [\phi^+(ij)^* v(ij) \psi^+(ij) + \phi^-(ij)^* v(ij) \psi^-(ij)]}{\int d\vec{x}_i \int d\vec{x}_j [\phi^+(ij)^* \psi^+(ij) + \phi^-(ij)^* \psi^-(ij)]} , \tag{17}$$

where

$$\phi^{\pm}(ij) = \frac{1}{\sqrt{2}} [\phi_i(i)\phi_j(j) \pm \phi_i(j)\phi_j(i)] . \tag{18}$$

In the Hartree-Fock approximations U_0 is given by

$$U_0 = \sum_{j \neq (i)} [U_{0\uparrow\uparrow}(ij)\delta_{\uparrow\uparrow, ij} + U_{0\uparrow\downarrow}(ij)\delta_{\uparrow\downarrow, ij}] , \tag{19}$$

where

$$U_{0\uparrow\uparrow}(ij) = \left(\frac{\alpha^2}{\pi}\right)^{-3/2} \frac{\int d\vec{x}_i \int d\vec{x}_j \phi^-(ij)^* v(ij) [\delta(\vec{x}_i - \vec{R}_i) + \delta(\vec{x}_i - \vec{R}_j)] \psi^-(ij)}{\int d\vec{x}_i \int d\vec{x}_j \phi^-(ij)^* \psi^-(ij)} , \tag{20}$$

and

$$U_{0\uparrow\downarrow}(ij) = \left(\frac{\alpha^2}{\pi}\right)^{-3/2} \frac{\int d\vec{x}_i \int d\vec{x}_j [\phi^+(ij)^* v(ij) \psi^+(ij) + \phi^-(ij)^* v(ij) \psi^-(ij)] [\delta(\vec{x}_i - \vec{R}_i) + \delta(\vec{x}_i - \vec{R}_j)]}{\int d\vec{x}_i \int d\vec{x}_j [\phi^+(ij)^* \psi^+(ij) + \phi^-(ij)^* \psi^-(ij)]} . \tag{21}$$

Because particle i spends $\frac{1}{2}$ of its time at lattice site i and the other half of its time at lattice site j, we insert two δ functions in evaluating U_0 as in Eq. (20) and Eq. (21). In fact, both δ functions give the same contribution to U_0. In Eqs. (16), (17), (20), and (21) $\psi^{\pm}(ij)$ is the correlated pair wave function obtained by solving the "Hartree-Fock" Bethe-Goldstone equation; i.e.,

$$\left\{ T(\vec{R}) + T(\vec{r}) + v(\vec{r}) + \frac{\hbar^2}{m} \alpha^4 (\vec{R} - \vec{d})^2 + \frac{1}{4} \frac{\hbar^2}{m} \alpha^4 [(\vec{r} - \vec{\Delta})^2 |_{z>0} + (\vec{r} + \vec{\Delta})^2 |_{z<0}] \right\} \psi^{\pm}(ij) = (\epsilon_{ij}^{\pm} - 2U_0)\psi^{\pm}(ij) \tag{22}$$

or

$$\left[T(\vec{R}) + T(\vec{r}) + v(\vec{r}) + \frac{\hbar^2}{m} \alpha^4 (\vec{R} - \vec{d})^2 + \frac{1}{4} \frac{\hbar^2}{m} \alpha^4 (r^2 + \Delta^2 - 2\Delta |z|) \right] \psi^{\pm}(ij) = (\epsilon_{ij}^{\pm} - 2U_0)\psi^{\pm}(ij) . \tag{23}$$

The single-particle potential in this equation is $\frac{1}{2}k(\vec{r} - \vec{\Delta})^2$ for $z > 0$ (particle 1 to the right of particle 2) and $\frac{1}{2}k(\vec{r} + \vec{\Delta})^2$ for $z < 0$ (particle 1 to the left of particle 2). For the kind of compact wave functions we seek to describe the solid, the "cusp" at $z = 0$ is of no consequence. Here we use the center-of-mass and relative coordinates

$$\begin{aligned} &\vec{r} = \vec{x}_j - \vec{x}_i , \quad \vec{\Delta} = \vec{R}_j - \vec{R}_i , \\ &\vec{R} = \tfrac{1}{2}(\vec{x}_j + \vec{x}_i) , \quad \vec{d} = \tfrac{1}{2}(\vec{R}_j + \vec{R}_i) , \end{aligned} \tag{24}$$

and

$$z = \vec{r} \cdot \hat{x} . \tag{25}$$

As in the Hartree case, we use the Hartree-Fock equations in two ways: (a) We solve Eq. (23) for $\psi^{\pm}(ij)$ variationally after decomposing $\psi^{\pm}(ij)$ into its partial waves. The state-dependent Reid soft-core potentials can only be studied in this kind of complicated partial-wave treatment. (b) We also treat $\psi^{\pm}(ij)$ in the cutoff approximation of Eq. (13). When $r_0 = 0$ in the cutoff approximation we have $g(r) = 1$ and $\psi^{\pm}(ij) = \phi^{\pm}(ij)$. The problem that results in this limit we refer to as the "Hartree-Fock problem." When $g(r)$ is given by $\theta(r - r_0)$ for $r_0 \neq 0$ we refer to the problem that results as the "correlated Hartree-Fock problem." When $g(r)$ is given by solving Eq. (23) we refer to this problem as the "Hartree-Fock t-matrix problem."

The formulas in this section are schematic as they do not include the angular momentum and spin dependence of the wave functions. In Appendix A we exhibit the formulas for U and U_0 that result from using a partial-wave decomposition of the wave function. The Appendix also contains details of how we handle the spin quantization problem.

III. RESULTS AND DISCUSSION

In this section we report the results of calculations using the sets of equations outlined above. There are three important elements to be discussed for each calculation: (a) the self-consistency condition, (b) the energy per particle, and (c) the qualitative properties of the physical state that results. In general we have done calculations at densities of 5×10^{14}, 16×10^{14}, and 50×10^{14} g/cm^3 for a bcc crystal structure with an antiferromagnetic spin configuration.[16]

A. Hartree calculations with $v_R(r)$

The self-consistency condition for α^2 in all cases can be written in the form

$$\alpha_{\text{comp}}{}^2 \equiv \frac{4}{3}\frac{m}{\hbar^2}\left[\overline{U}(\alpha^2) - U_0(\alpha^2)\right] , \tag{26}$$

where $\overline{U}$ and U_0 are computed as functions of α^2 using equations specific to the particular approximation being employed. We denote by $\alpha_{SC}{}^2$ the self-consistent value of α^2 which occurs when $\alpha_{\text{comp}}{}^2$ equals α^2. The results of this kind of procedure for the "Hartree problem" [$r_0 = 0$ in Eq. (13)] are shown in Figs. 1(a), 1(b), and 1(c) in which we plot $\alpha_{\text{comp}}{}^2$ vs α^2 for the three densities we explored. A self-consistent value of α^2 is found when the $\alpha_{\text{comp}}{}^2$ curve crosses the self-consistency line ($\alpha_{\text{comp}}{}^2 = \alpha^2$) drawn in the figures. Self-consistent values of α^2 are found for all three densities in this "Hartree problem." The energy per particle of the system is shown in Figs. 2(a), 2(b), and 2(c) as a function of α^2 for these densities. As $\alpha^2 \to 0$ the energy per particle approaches the Hartree liquid value (the value corresponding to $\alpha^2 = 0$),[15]

$$E_L^R = \frac{1}{2}\frac{N}{V} 4\pi \int_0^{+\infty} r^2 dr\, v_R(r)$$

$$= \frac{3}{2}\frac{A}{\beta^2}\frac{1}{r_S{}^3} , \tag{27}$$

where $A = 6484.2$ MeV, $\beta = 7$, and r_S is defined by

$$\frac{V}{N} = \tfrac{4}{3}\pi \frac{r_S{}^3}{\mu^3} , \tag{28}$$

where $\mu = 0.7$ F^{-1}. These asymptotic values of the energy are noted on the left-hand sides of Figs. 2(a), 2(b), and 2(c). For each of the three densities, we see that the energy per particle approaches its corresponding liquid value rapidly for $\alpha^2 < 1$. On these figures we note that the energies corresponding to $\alpha_{SC}{}^2$, the self-consistent value of α^2 found from Figs. 1(a), 1(b), and 1(c), fall very close to their corresponding energy minima. This becomes particularly true as the density is increased and the relevant $\alpha_{SC}{}^2$ becomes larger.[17] In Fig. 3 we show $\alpha_{SC}{}^2\Delta^2$ as a function of density. We regard this parameter $\alpha_{SC}{}^2\Delta^2$ as a reasonable estimate of the qualitative structure of the solid.[12] It is a measure of the ratio of the wave-function width to the interparticle spacing. We note that at the lowest density $\rho = 5\times10^{14}$ g/cm^3, $\alpha_{SC}{}^2\Delta^2 = 12.3$. In Fig. 4 we show a second test of the qualitative structure of the wave function (see Pandharipande, Ref. 5). This is the "number of particles per particle," i.e.,

$$n = \tfrac{4}{3}\pi(\langle u^2\rangle)^{3/2}\frac{N}{V}$$

$$= \frac{0.63}{\alpha^3 r_S{}^3} , \tag{29}$$

where $\vec{u}$ is the displacement of a particle away from its lattice site. The number n is the volume of the single-particle wave function times the density of particles. It is a measure of the average number of particles in the volume occupied by a particle. For a solid we want this number to be much less than 1. For each density we define $\alpha_C{}^2$ as the value of α^2 for which $n = 1$ and note it on the self-consistency plots in Figs. 1(a), 1(b), and 1(c) and on similar plots below. We regard values of α^2 less than $\alpha_C{}^2$ as describing a liquid-like state or as unphysical.

In Figs. 1(a), 1(b), and 1(c) and Figs. 2(a), 2(b),

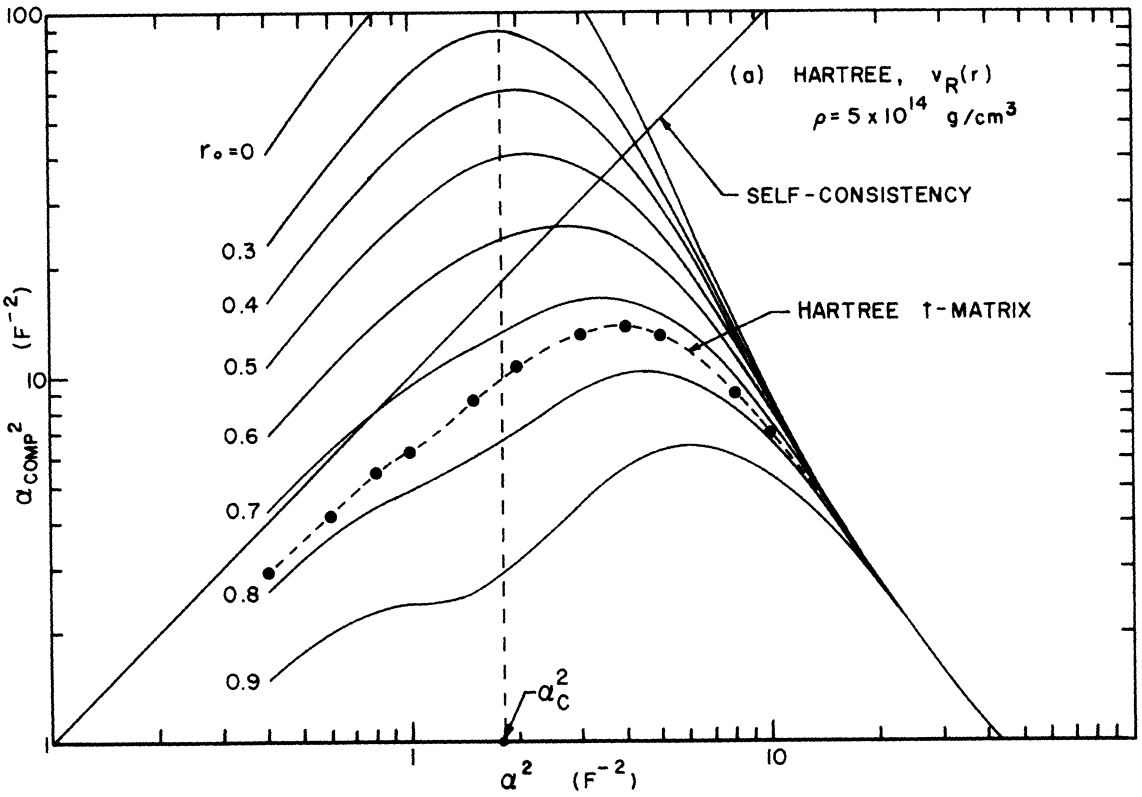

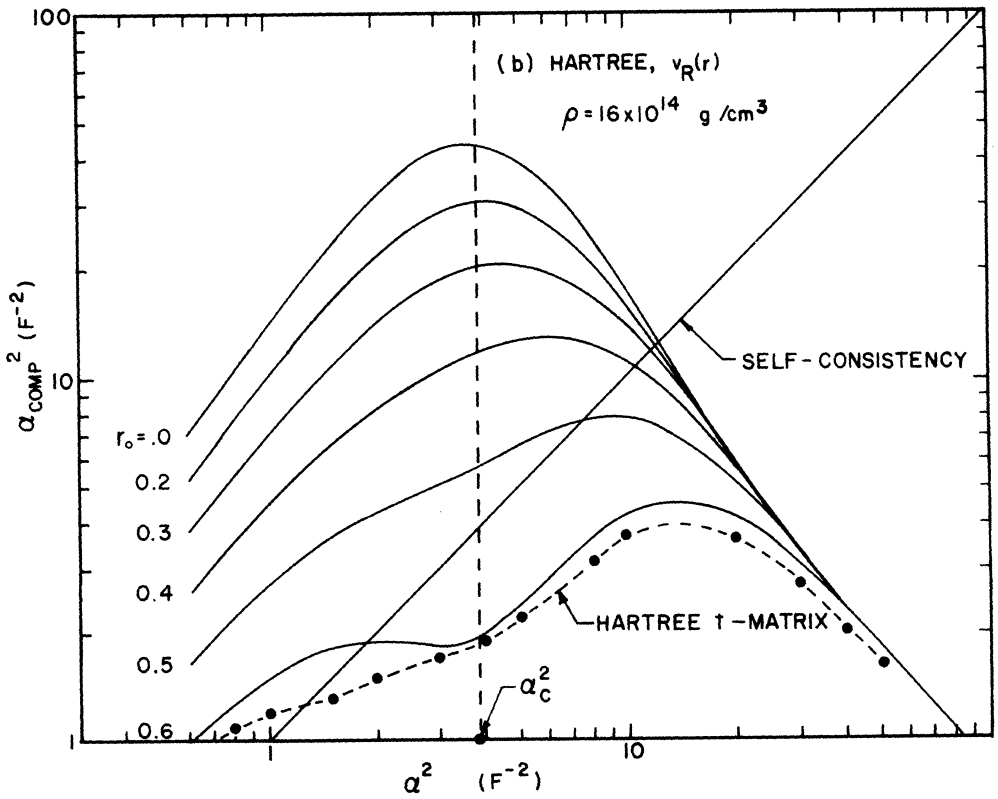

FIG. 1. *(Continued on following page)*

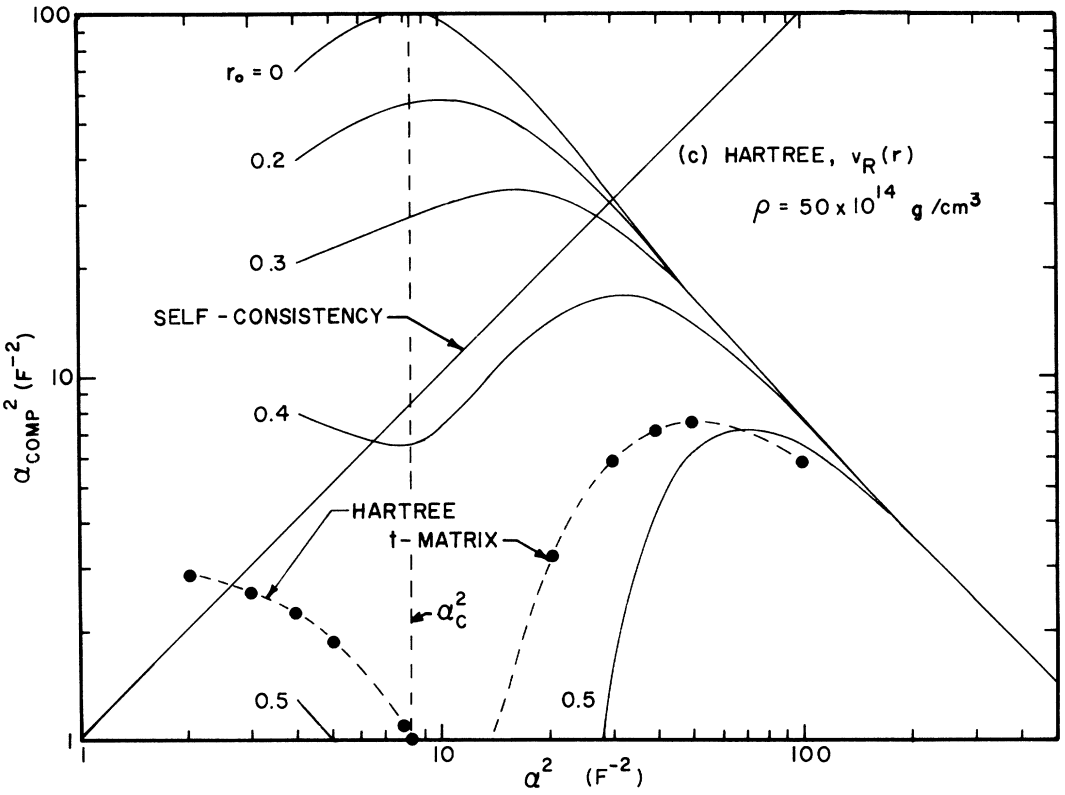

FIG. 1. Hartree self-consistency condition for $v_R(r)$. For the 3 densities we show α_{comp}^2 calculated from Eq. (26) as a function of α^2 for the Hartree ($r_0=0$), correlated Hartree ($r_0 \neq 0$), and Hartree t-matrix calculations. The physical region is $\alpha^2 \geq \alpha_c^2$. Self-consistency is achieved when the value of α_{comp}^2 crosses the diagonal labeled "self-consistency." The Hartree t-matrix results are similar to those obtained with $0.7 \leq r_0 \leq 0.8$ at 5×10^{14} g/cm^3, $r_0 \approx 0.6$ at 16×10^{14} g/cm^3, and $r_0 \approx 0.5$ at 50×10^{14} g/cm^3. There is no self-consistency in the physical region for the larger values of r_0 or for the Hartree t-matrix results.

and 2(c) we also show the corresponding results for the self-consistency condition and for the energy per particle calculated for the "correlated Hartree problem" [$r_0 \neq 0$ in Eq. (13)] as a family of curves for varying r_0 values. As with the "Hartree problem" above, the values of the energy per particle in this "correlated Hartree" calculation approach their corresponding liquid values as $\alpha^2 \to 0$. We have

$$E_L^R(r_0) = E_L^R(1 + \beta r_0 \mu) e^{-\beta r_0 \mu} . \tag{30}$$

We note that E/N approaches this asymptotic value rapidly as $\alpha^2 \to 1$ for all cases. This is particularly true for the larger values of r_0. The reason for this is that as $r_0 \to 1$ F the wave function need not spread very far before a particle has seen all there is of the interaction. Thus the liquid limit is achieved for rather large values of α^2 for the larger values of r_0. From Fig. 1(a), for a density of 5×10^{14} g/cm^3, we see that as the cutoff becomes larger the values of α_{comp}^2 become less until at $r_0 = 0.7$ F, α_{SC}^2, the self-consistent value of α^2, becomes less than the critical value, α_c^2. Thus the self-consistent wave functions become unphysically large for $r_0 \gtrsim 0.7$ F. We further note in Fig. 2(a) that the energy ceases to have a minimum as a function of α^2 for $r_0 \gtrsim 0.7$ F. The physics in these results is simple. The self-consistency condition requires that a Hartree calculation of the structure of the single-particle well leads to a single-particle well that will yield the Hartree single-particle wave function. As r_0 becomes large the repulsive part of the interaction becomes so weak that the neighbors of a particle cannot suitably localize it in space to produce the Hartree wave function. Qualitatively similar results are obtained for the other two densities as shown in Figs. 1(b), 1(c), 2(b), and 2(c). We next show that the behavior of α_{comp}^2 as a function of α^2 for the "Hartree t-matrix" pair wave function is much the same as that found here for the cutoff correlation functions.

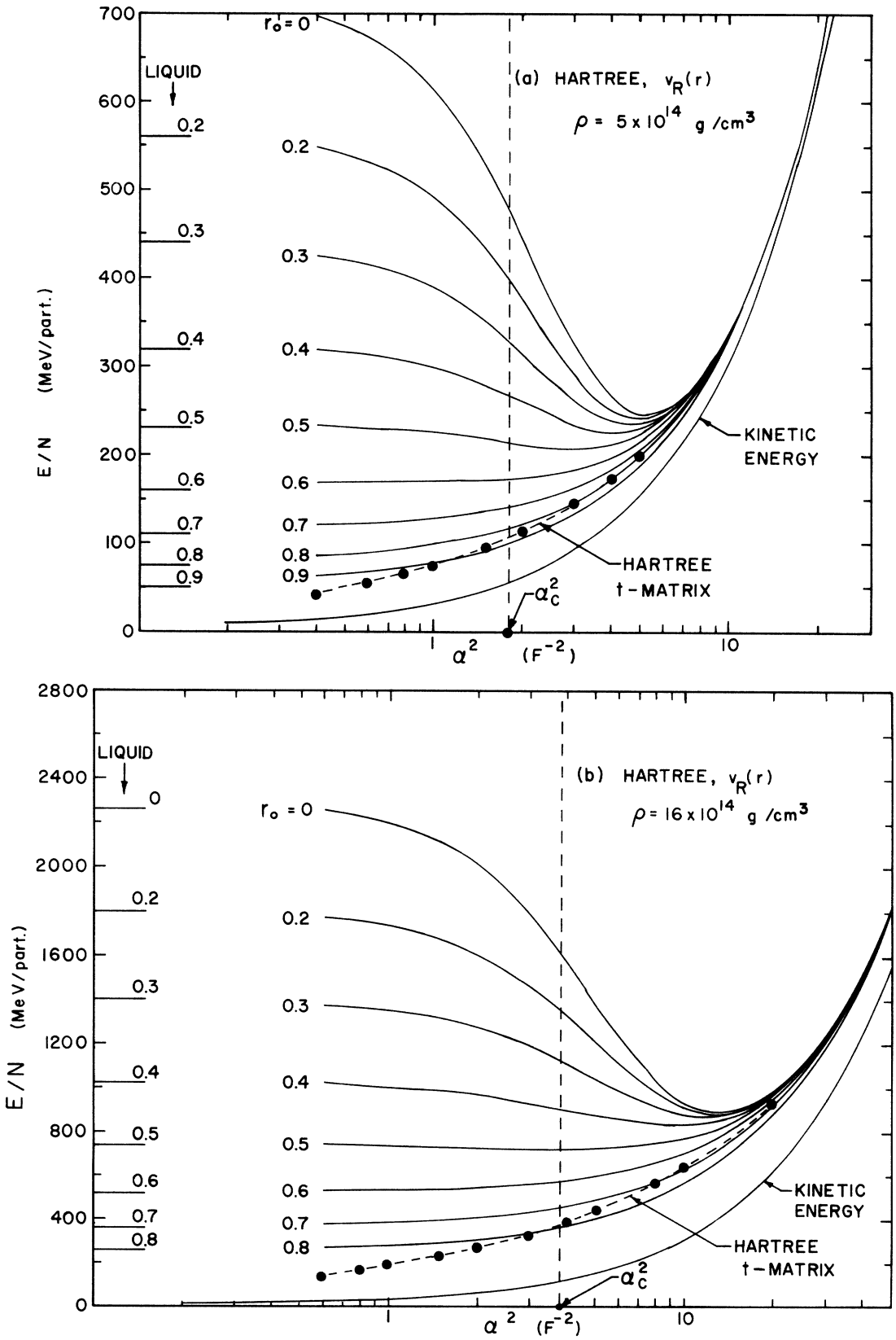

FIG. 2. *(Continued on following page)*

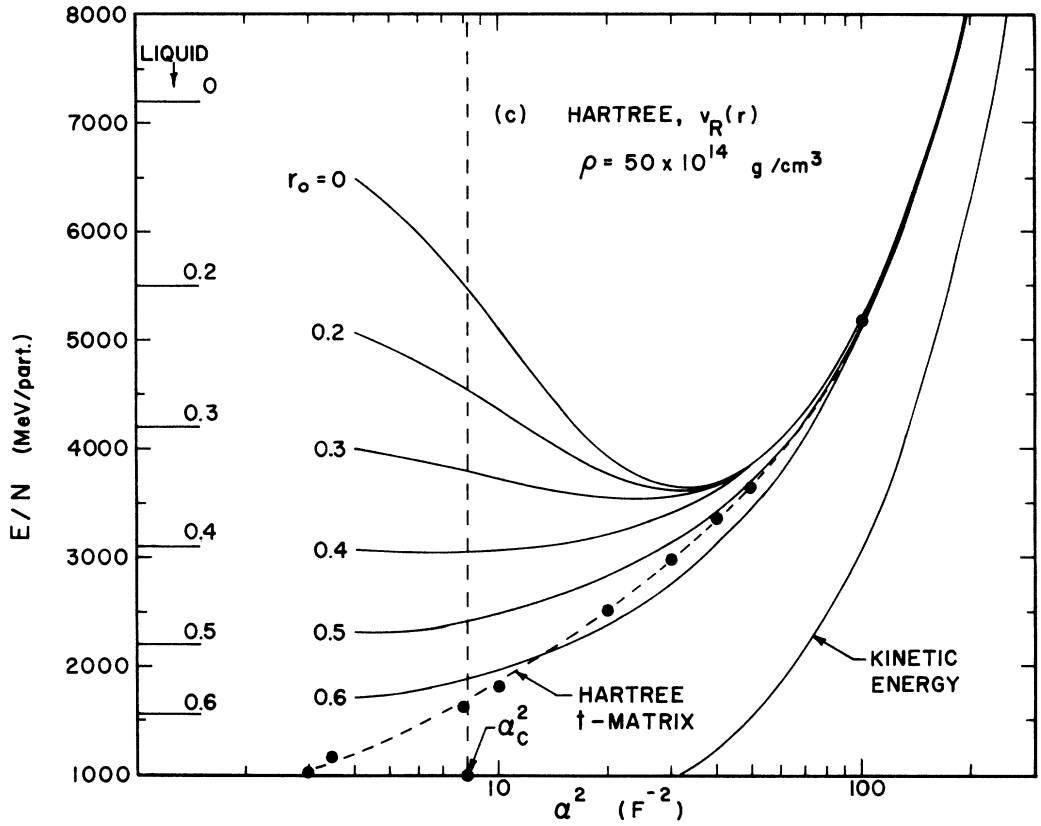

FIG. 2. Hartree energy per particle for $v_R(r)$. For the 3 densities we show E/N vs α^2 for the Hartree ($r_0 = 0$), correlated Hartree ($r_0 \neq 0$), and Hartree t-matrix calculations. On the left-hand side we show the Hartree liquid energy values. The energy per particle approaches these liquid values as $\alpha^2 \to 0$. For $r_0 > 0.5$ the Hartree energy at $\alpha^2 \lesssim 1.0$ is already nearly equal to the liquid value. For large α^2 the kinetic energy dominates the total energy. The potential energy is independent of α^2 for large α^2 where it is given by a lattice sum. We note that a minimum in E/N vs α^2 occurs for smaller values of r_0; so does self-consistency. The existence of a self-consistent α^2 or a minimum in E/N seem to be related. We note that for the physical valuesof α^2 the energy per particle given by the Hartree t-matrix is about the same as a simple cutoff.

In Figs. 1(a), 1(b), 1(c), 2(a), 2(b), and 2(c) we also show the results of a Hartree t-matrix calculation in which the correlation function is found from the solution to Eq. (10). The computational procedure in this case involves an intermediate step: (1) Choose an α^2, (2) solve the differential equation for the correlation function appropriate to α^2, and (3) calculate $\alpha_{\text{comp}}{}^2$ using the correlation function from step (2). In Figs. 1(a), 1(b), and 1(c) we exhibit the results of such a t-matrix analysis of the self-consistency condition. We see that for large values of α^2, $\alpha_{\text{comp}}{}^2$ is the same as the Hartree values. For large α^2 the correlation function when combined with $v_R(r)$ to yield a t matrix leads to an insubstantial change in the interaction in the region of space where the particles are localized. For 5×10^{14} g/cm^3 as $\alpha^2 \to 10$ the wave function has broadened enough that the particles sample the region of space where the t matrix differs from $v_R(r)$ and $\alpha_{\text{comp}}{}^2$ differs from the Hartree value of $\alpha_{\text{comp}}{}^2$. From Fig. 1(a) we see that $\alpha_{\text{comp}}{}^2$ follows a curve midway between that appropriate to $g(r)$ cut off at $r_0 = 0.7$ and $r_0 = 0.8$. That is, the effect of introducing the t matrix determined by solving Eq. (10) is equivalent to a $g(r)$ cutoff at $0.7 \lesssim r_0 \lesssim 0.8$. We note further that *no self-consistent α^2 is found* with $g(r)$ from Eq. (10) except possibly far into the unphysical region. The similarity of $\alpha_{\text{comp}}{}^2$ calculated with the exact t matrix to $\alpha_{\text{comp}}{}^2$ calculated with a cutoff potential permits us to repeat the explanation given earlier. The correct t matrix for $v_R(r)$ leads to too weak an effective interaction to permit self-consistent binding of the particles. Furthermore, as shown in Fig. 2(a), no energy minimum is found in the physical region. We find

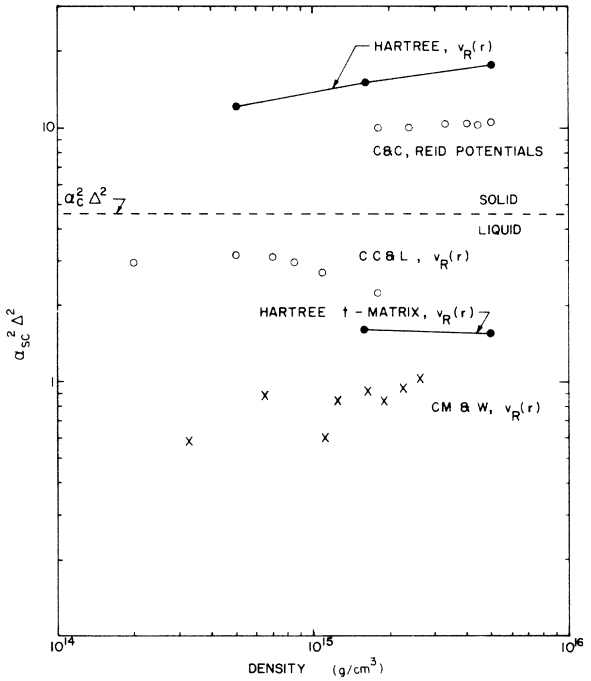

FIG. 3. $\alpha_{SC}{}^2\Delta^2$ vs density. The value of $\alpha_{SC}{}^2\Delta^2$ is shown as a function of density for several calculations: $v_R(r)$ in the Hartree and Hartree t-matrix approximation, the calculation of Canuto and Chitre on the full Reid potentials, the calculation of Canuto, Chitre, and Lodenquai on $v_R(r)$ and the calculation of Chakravarty, Miller, and Woo on $v_R(r)$. The unphysical region or liquid region is at $\alpha_{SC}{}^2\Delta^2 \leq 4.6$. Most calculations lead to unphysical wave functions.

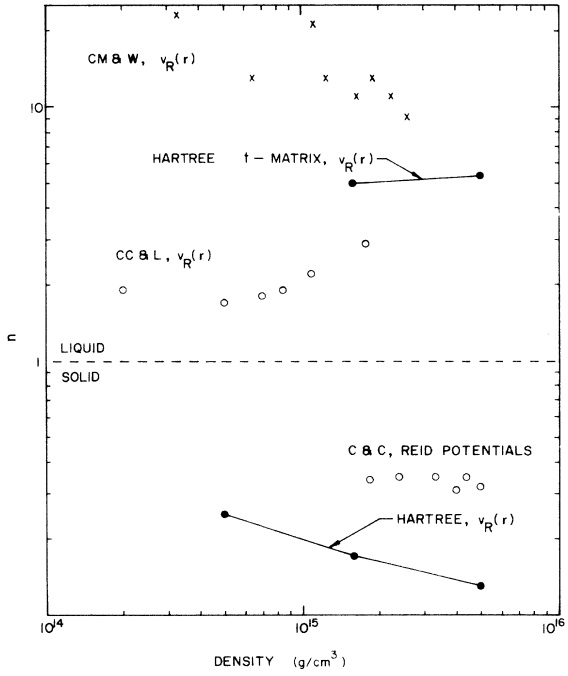

FIG. 4. n vs density. The value of n given by Eq. (29) is shown as a function of density for the calculations discussed in the text. See the caption to Fig. 3 for an enumeration. For $n>1$ the wave function is highly unphysical for a solid; i.e., it is liquidlike. The result of most solid calculations lies in the liquid region.

these results at all densities. We find at most a self-consistency in the highly unphysical region at higher densities. The corresponding values of $\alpha_{SC}{}^2\Delta^2$ and n, when available, are recorded on Figs. 3 and 4 for comparison with the Hartree results.

We note that in solving the "Hartree t-matrix problem" with $g(r)$ given by Eq. (10) we find values $\alpha_{SC}{}^2$ and E/N similar to those found by Canuto, Chitre, and Lodenquai. As we have solved Eq. (10) in the one-dimensional approximation of Guyer and Sarkissian,[15] which we do not completely trust as $\alpha^2 \to \alpha_C{}^2$, we expect the results of Canuto, Chitre, and Lodenquai to be more accurate than our own. If the self-consistent values of α^2 were larger, we would expect excellent agreement between the two calculations. Thus our results here are qualified by the fact that we have used the one-dimensional approximation of Guyer and Sarkissian. We believe this to be an excellent approximation in the physical region. Below we discuss the Hartree-Fock solutions in which the one-dimensional approximation is removed.

B. Hartree-Fock calculations with $v_R(r)$

For a Hartree-Fock calculation of the ground-state energy for an antiferromagnetic spin arrangement, the self-consistency results are shown in Figs. 5(a), 5(b), and 5(c) and the corresponding energy per particle results are shown in Figs. 6(a), 6(b), and 6(c). The results shown in these figures include those for the "Hartree-Fock problem," the "correlated Hartree-Fock problem," and the "Hartree-Fock t-matrix problem." We note that as $\alpha^2 \to 0$ the energy per particle approaches $\frac{1}{2}$ of the energy per particle of the Hartree liquid; i.e., it goes to the Hartree-Fock liquid value.[15] Comparing Figs. 1(a), 1(b), and 1(c) with Figs. 5(a), 5(b), and 5(c) and Figs. 2(a), 2(b), and 2(c) with Figs. 6(a), 6(b), and 6(c), we see that as α^2 becomes large the Hartree-Fock value of $\alpha_{\rm comp}{}^2$ approaches the Hartree value of $\alpha_{\rm comp}{}^2$ and the energy per particle approaches the energy per particle of the Hartree calculation. But as $\alpha^2 \to \alpha_C{}^2$ we find $\alpha_{\rm comp}{}^2$ goes through zero and becomes negative. Negative values of $\alpha_{\rm comp}{}^2$ can occur at large α^2 with a potential having an attractive region. In that case, for a suitably large

lattice spacing, a particle sits on an equilibrium site in a potential at higher energy than the average potential energy nearby. This is the classic situation for a quantum crystal or for neutrons in the $v_{^1S_0}(r)$ potential at low density. At the opposite extreme $\alpha^2 \to \alpha_c^2$, however, a different effect occurs to cause α_{comp}^2 to become negative. As $\alpha^2 \to \alpha_c^2$ the Hartree-Fock values of the energy per particle deviate strongly from the Hartree values and begin to approach the Hartree-Fock liquid energy. In Figs. 7(a) and 7(b) we show separately the behavior of $\overline{U}$ and U_0 for the Hartree and Hartree-Fock calculation for a density of 5×10^{14} g/cm^3. We see that $\overline{U}$ and U_0 are the same for large α^2 in both the Hartree and Hartree-Fock calculations. As $\alpha^2 \to \alpha_c^2$ the Hartree-Fock value of $\overline{U}$ deviates more rapidly from the Hartree value of $\overline{U}$ than the Hartree-Fock value of U_0 deviates from the Hartree value of U_0. Thus the average potential energy of a particle near a lattice site becomes smaller, due to the spin correlations that drive the opposite spin particles away, more rapidly than the potential energy of the particle at the lattice site. When a particle is fixed on a lattice site its relative motion with respect to its neighbors is described by $\exp[-\alpha^2(\vec{r}-\vec{\Delta})^2]$ and it has less overlap with its neighbors than when it is free to move and its relative motion is described by $\exp[-(\alpha^2/2)(\vec{r}-\vec{\Delta})^2]$. Thus the Pauli principle affects the average potential energy more strongly, for fixed α^2, than it does the lattice -site potential energy.

In Figs. 5(a), 5(b), 5(c), 6(a), 6(b), and 6(c) we also show the results of a Hartree-Fock t-matrix calculation employing a partial-wave decomposition of the pair wave function and an antiferromagnetic spin arrangement. As with the Hartree t-matrix calculation described above, an intermediate step of solving the pair equation, in this case Eq. (23), is involved. In the Hartree-Fock case a partial-wave decomposition of the pair equation is required. This decomposition leads to separate systems of coupled equations for the even and odd angular momentum components. The total even and odd wave functions are jointly normalized. (The question of normalization is an important one and is discussed in Appendix C.) The systems of coupled equations are solved variationally. For the self-consistency condition we find the results shown in Figs. 5(a), 5(b), and 5(c). For relatively large values of α^2, α_{comp}^2 becomes greater than the Hartree values because of the limit on the number of partial waves we include. (See the remarks in Appendix B.) At intermediate values of α^2, α_{comp}^2 agrees well with the results of the Hartree t-matrix calculations which are also plotted in these figures. Then at $\alpha^2 \approx \alpha_c^2$, α_{comp}^2 begins to deviate from the Hartree results and to follow the trend noticed in the "correlated Hartree-Fock" calculations described above. As in that case no self-consistency is achieved in the physical region. We see that the behavior of α_{comp}^2 in the full Hartree-Fock t-matrix calculation is essentially the same as in the Hartree t-matrix calculation in the physical region. The t matrix behaves like a cutoff at some value of r_0. As $\alpha^2 \to 0$ the effective cutoff moves to larger r_0 so that α_{comp}^2 does not necessarily follow a single r_0 curve.

C. Hartree calculations with $v_{^1S_0}(r)$

In Figs. 8 and 9 we illustrate the results obtained from a Hartree solution for the $v_{^1S_0}(r)$ model potential. The results shown in these figures include those for the "Hartree," the "correlated Hartree," and the "Hartree t-matrix" problems. The general behavior of these results are strikingly similar to the Hartree results we have just discussed for the $v_R(r)$ model potential at the three densities we have studied—5×10^{14}, 16×10^{14}, and 50×10^{14} g/cm^3. For this reason, we only present the intermediate density results. The introduction of a strong attractive term (potential depth ≈ -90 MeV) into the state-independent model potential problem does not affect the general behavior of the α^2 self-consistency curves nor the E/N curves although the values of E/N are now typically much lower. The "Hartree t-matrix" results show no self-consistency and no energy minimum, except perhaps far into the unphysical region for all three densities we have studied.

D. Hartree-Fock calculations with $v_{^1S_0}(r)$

In Figs. 10 and 11 we illustrate the results obtained from a Hartree-Fock solution for the $v_{^1S_0}(r)$ model potential. The results shown in these figures include those for the "Hartree-Fock," the "correlated Hartree-Fock," and the "Hartree-Fock t-matrix" problems. Here again, the general behavior of these results are very similar to the Hartree-Fock results for the $v_R(r)$ model potential. Consequently, we only display the 16×10^{14} g/cm^3 results although our analysis extended to 5×10^{14} and 50×10^{14} g/cm^3. As α^2 becomes large the Hartree-Fock values of α_{comp}^2 and E/N approach their corresponding Hartree values. As α^2 gets smaller and approaches α_c^2, α_{comp}^2 deviates from its Hartree values. However, as α_{comp}^2 enters the unphysical realm ($\alpha_{\text{comp}}^2 < \alpha_c^2$) we observe an effect not previously observed in the $v_R(r)$ results. For the $v_R(r)$ Hartree-Fock results, α_{comp}^2 becomes negative in the unphysical

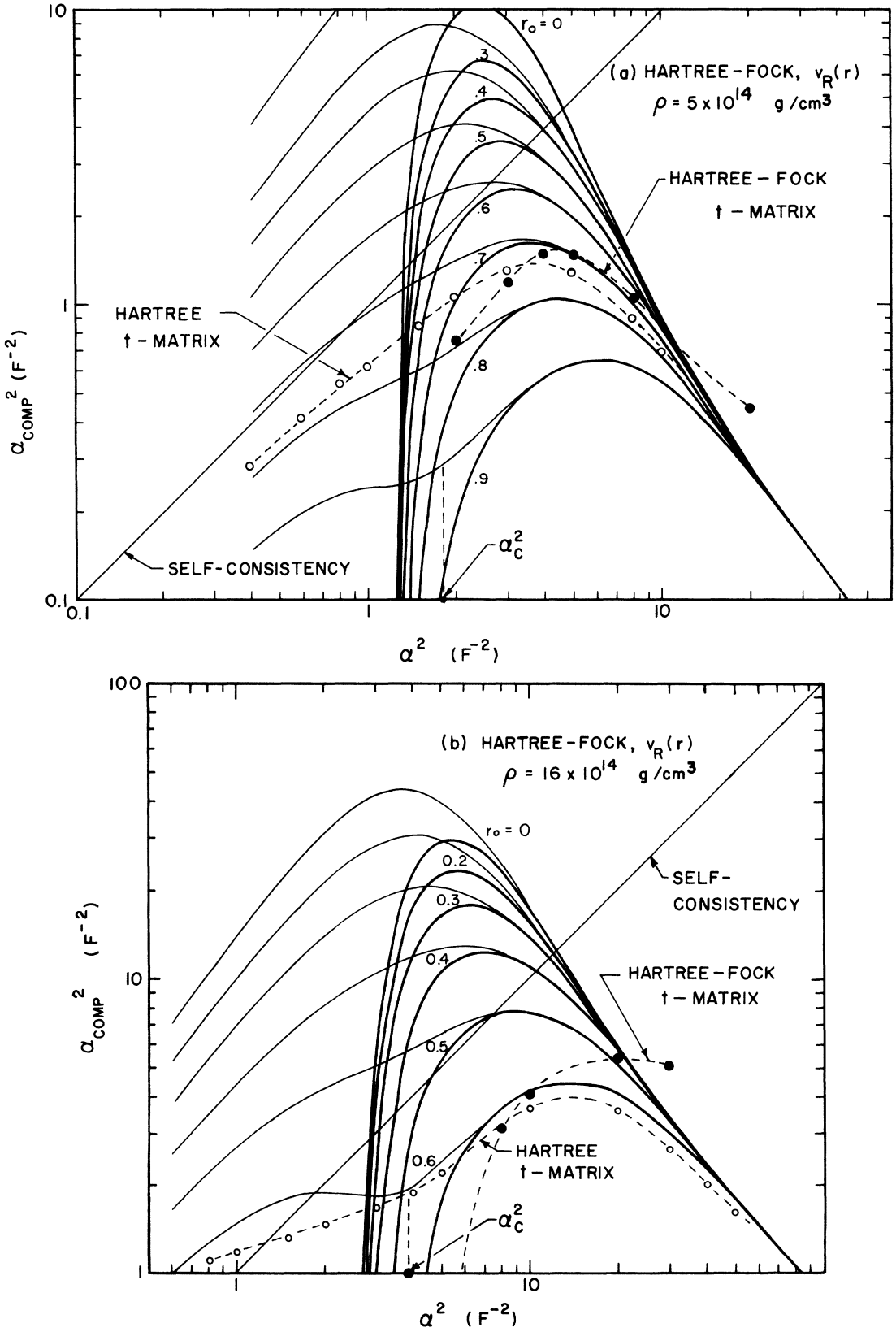

FIG. 5. *(Continued on following page)*

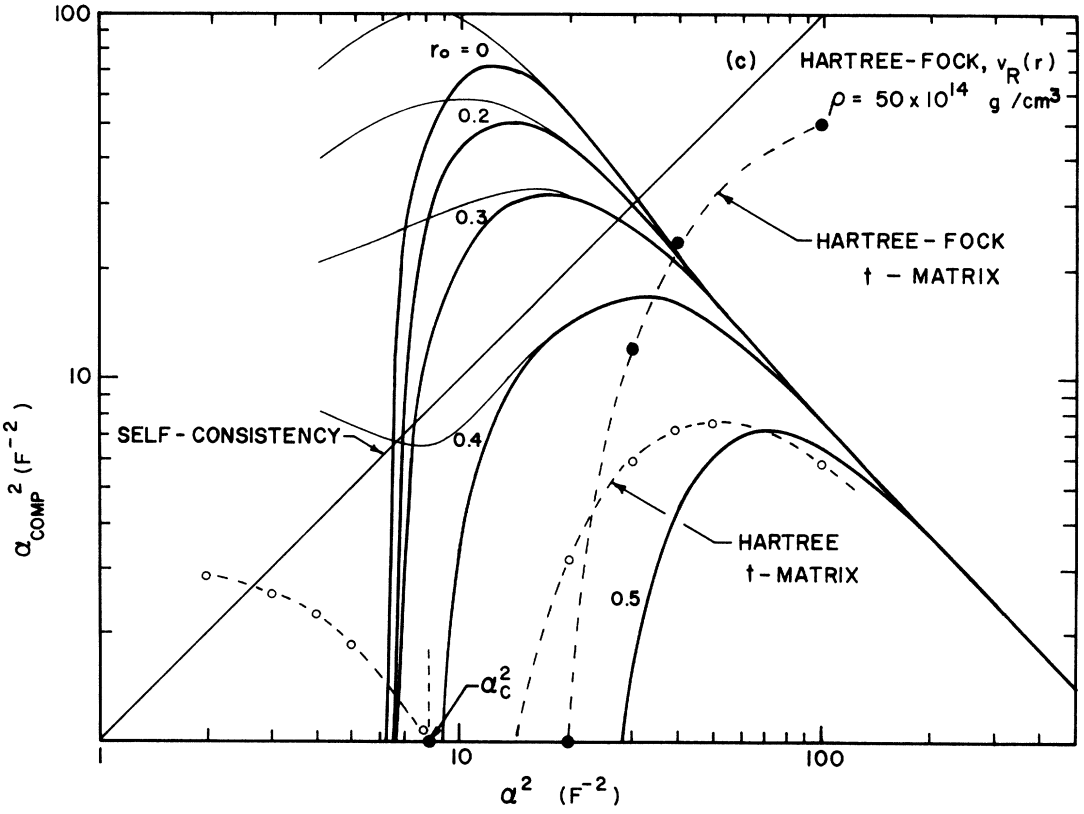

FIG. 5. Hartree-Fock self-consistency condition for $v_R(r)$. For the 3 densities we show α_{comp}^2 calculated from Eq. (26) as a function of α^2 for the Hartree-Fock, correlated Hartree-Fock, and Hartree-Fock t-matrix calculations. We also show the Hartree values of α_{comp}^2 (light curves) for comparison with the Hartree-Fock α_{comp}^2 (heavy curves) and the Hartree t-matrix result for comparison with the Hartree-Fock t-matrix result. The dip in the Hartree-Fock values of α_{comp}^2 is the manifestation of a zero on a log scale. On a linear scale the bumps and dips that appear here disappear. See the discussion involving Fig. 7 for an explanation of the zero in α_{comp}^2. The Hartree-Fock results are in all cases similar to the Hartree results for large α^2. As $\alpha^2 \to \alpha_C^2$ large overlap occurs and departure of the Hartree-Fock results from the Hartree sets in. There is no self-consistency in the Hartree-Fock t-matrix calculation.

region. For the $v_{^1S_0}(r)$ Hartree-Fock results, α_{comp}^2 becomes (or attempts to become) positive deep in the unphysical region. This reverse behavior of α_{comp}^2 arises from the peculiar behavior of the $\overline{U}$ and U_0 values for the Hartree-Fock calculations in the large overlap region for the $v_{^1S_0}(r)$ attractive potential. The "Hartree-Fock t-matrix" results show no self-consistency and no energy minimum except in the unphysical regime owing to the behavior just described. This behavior is also observed for $\rho = 5 \times 10^{14}$ g/cm^3. For $\rho = 50 \times 10^{14}$ g/cm^3 however, our analysis does not extend far enough into the small-α^2 unphysical region to determine whether self-consistency or an energy minimum exist. The corresponding values of $\alpha_{SC}^2 \Delta^2$ and n, where available, are plotted in Figs. 3 and 4, which clearly reveal their unphysical nature.

These results complete the series of calculations associated with the model problems. A number of conclusions are possible:

(a) The sequence of model problems defined by the potentials $v_R(r)$ and $v_{^1S_0}(r)$, the correlation functions $g(r) = \theta(r - r_0)$ for $r_0 = 0, 0.1, 0.2, \ldots$, the choice of a bcc geometry, the density range $5 \times 10^{14} \leq \rho \leq 50 \times 10^{14}$ g/cm^3, and the choice of an antiferromagnetic spin arrangement (when a spin arrangement is required) have well defined Hartree and Hartree-Fock solutions for suitably strong repulsive interactions.

(b) The asymptotic behavior of these solutions is in agreement with the expectations that follow from rather general physical arguments. Specifically, the Hartree and Hartree-Fock results are

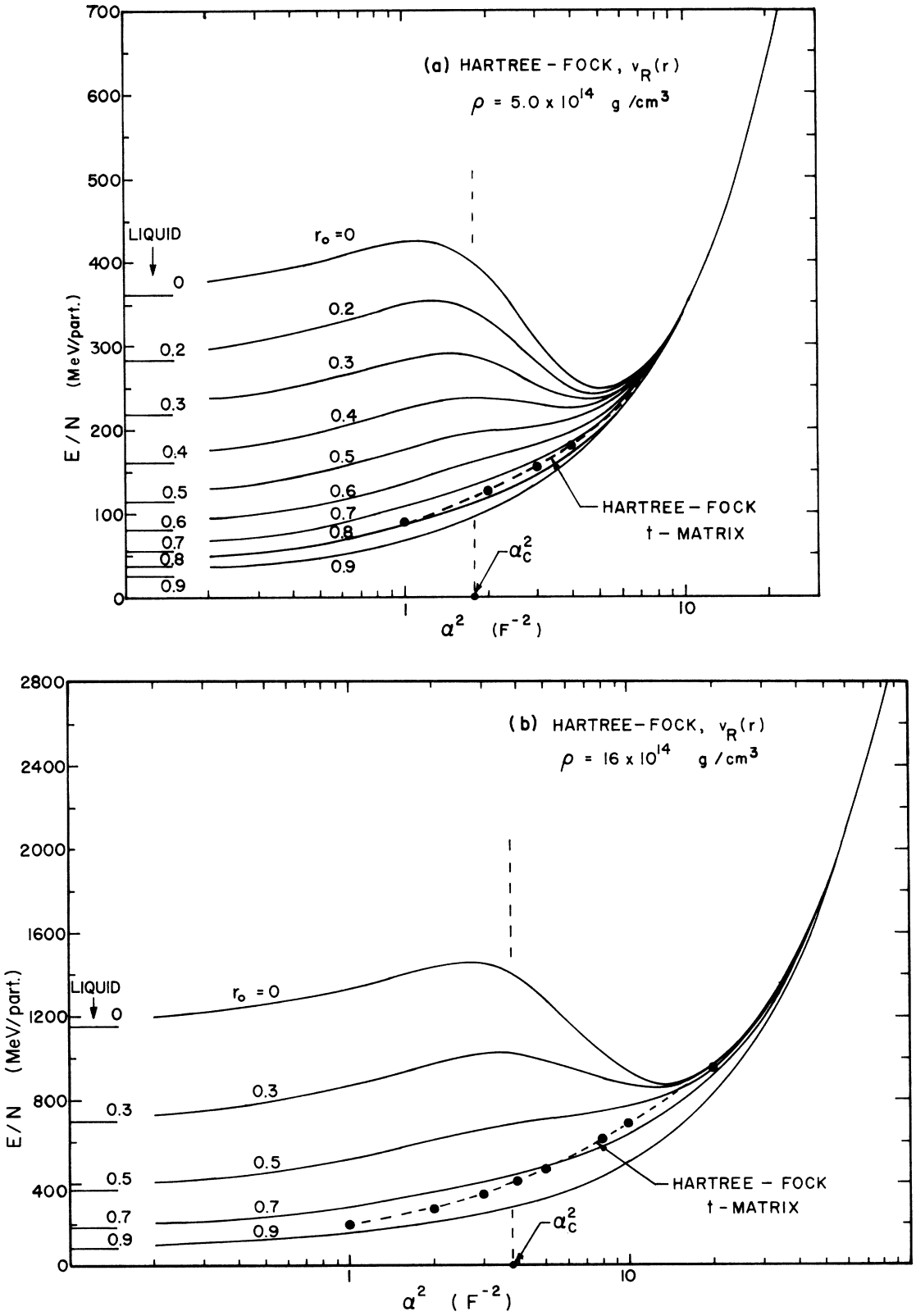

FIG. 6. *(Continued on following page)*

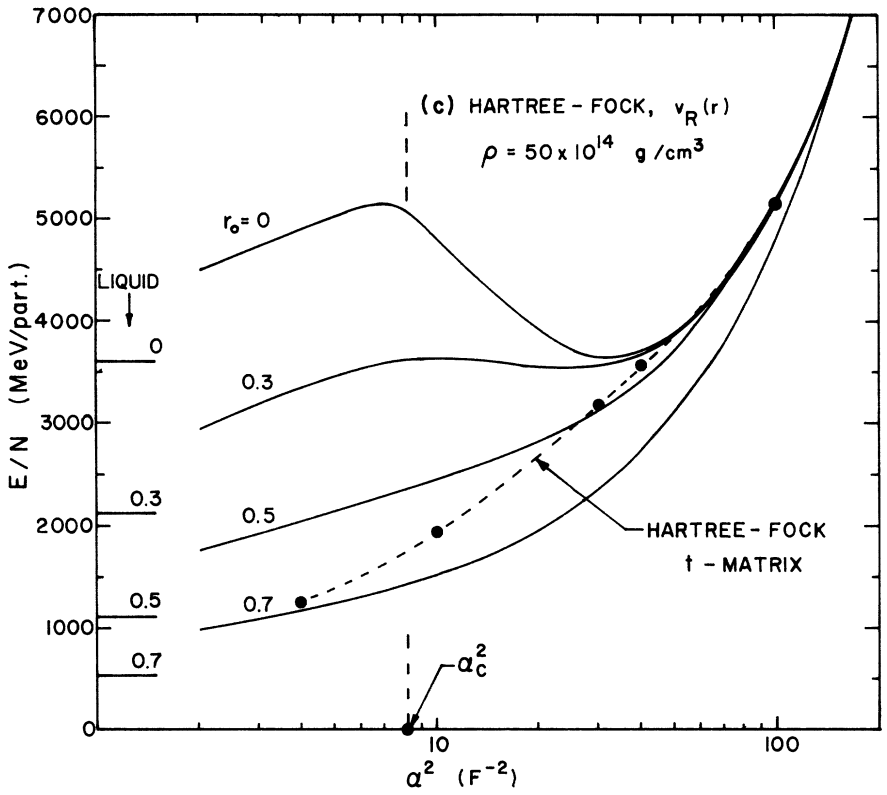

FIG. 6. The Hartree-Fock energy per particle for $v_R(r)$. For the 3 densities we show E/N vs α^2 for the Hartree-Fock, correlated Hartree-Fock, and Hartree-Fock t-matrix calculations. On the left-hand side we show $\frac{1}{2}$ of the Hartree liquid energies, i.e., the Hartree-Fock liquid energies. The Hartree-Fock energy curves follow the Hartree energy curves until $\alpha^2 \approx \alpha_c{}^2$ where the Pauli principle comes into play and the Hartree-Fock energy begins to approach the liquid value. For the Hartree-Fock t-matrix calculation the energy per particle is almost the same as the Hartree t-matrix energy per particle.

in agreement for small overlap, the Hartree and Hartree-Fock energies are asymptotically correct as the liquid limit is reached and the self-consistency condition breaks down as $\alpha^2 \to \alpha_c{}^2$ in a physically understandable way.

(c) The solution to the Hartree t-matrix problem with the correlation function given by Eq. (10) or the Hartree-Fock t-matrix problem with the correlation function given by Eq. (23) is not substantially different in detail or in final result from the solution of the model problems. Therefore, conclusions drawn from the discussion of the model problems described in (a) above are correct for the relatively complex Hartree t-matrix and Hartree-Fock t-matrix problems.

It remains to be seen whether the introduction of realistic potentials changes these conclusions. We believe that, as most of the important results follow from physical arguments invariant to the details of the potentials involved, the introduction of the full collection of Reid soft-core potential will not change the conclusions. In Sec. IV, we present our results using the full Reid soft-core potentials.

IV. THE FULL SOLID-NEUTRON-MATTER PROBLEM

In this section we discuss our results and understanding of the full solid-neutron-matter problem. In Figs. 12 and 13 we show the results of our Hartree-Fock t-matrix computations using the full set of Reid soft-core potentials. We present the $\alpha_{\text{comp}}{}^2$ and the energy as a function of α^2 for a density of 16×10^{14} g/cm^3. For comparison we also display the corresponding Hartree-Fock t-matrix results for the two state-independent model potentials $v_R(r)$ and $v_{^1S_0}(r)$. The self-consistent results of Canuto and Chitre at this density are plotted as single points on each figure. In Fig. 12 the data in the region $\alpha^2 > 10$ are unreliable because of the insufficient number of partial waves

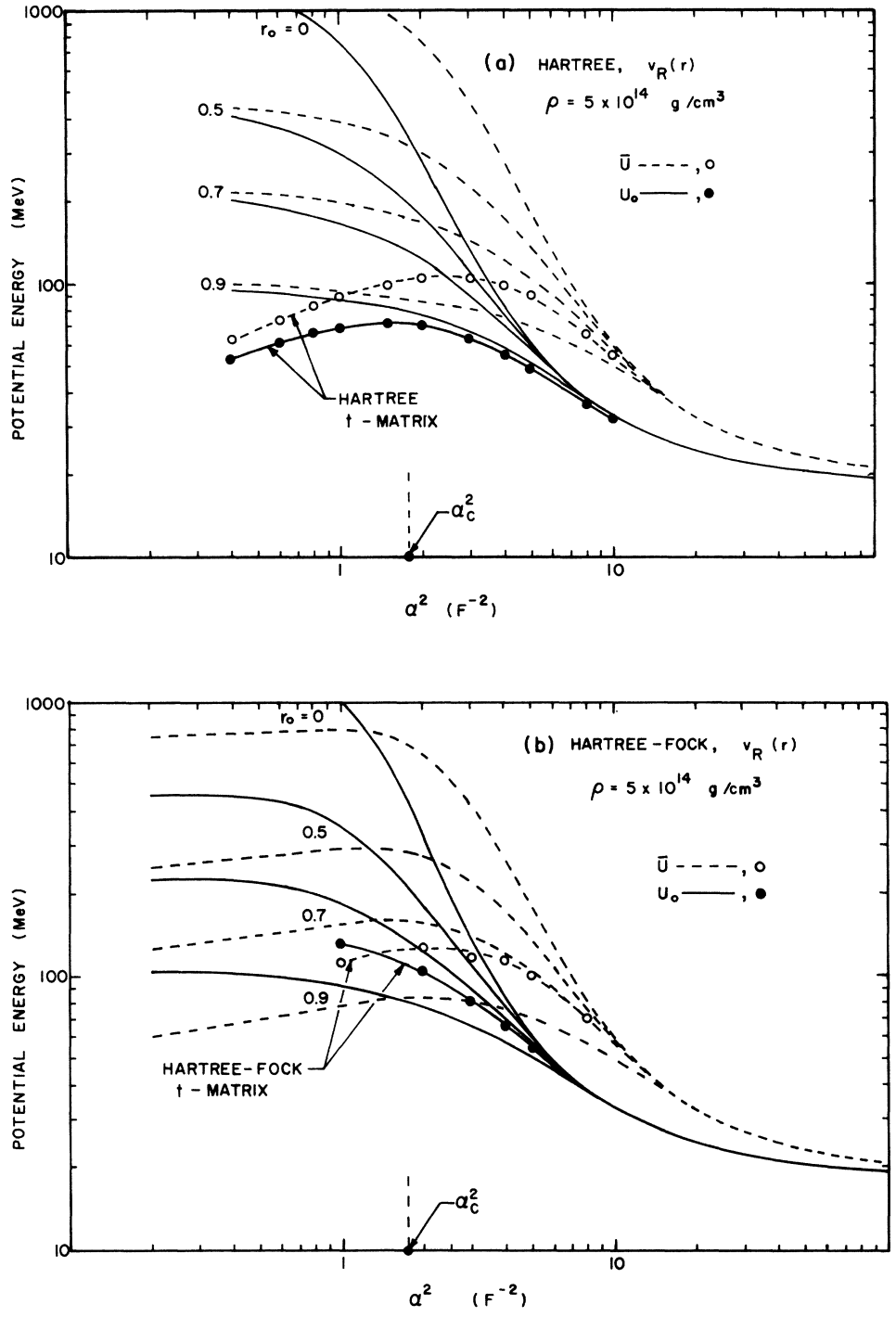

FIG. 7. $\bar{U}$ and U_0 as a function of α^2. To understand the behavior of $\alpha_{\text{comp}}{}^2$ in the Hartree and Hartree-Fock calculations we show $\bar{U}$ and U_0 for a number of cases. In (a) we show $\bar{U}$ and U_0 for the Hartree calculations; in (b) we show $\bar{U}$ and U_0 for the Hartree-Fock calculations. We note that for large α^2, $\bar{U}(2\alpha^2) = U_0(\alpha^2)$ and the Hartree and Hartree-Fock values of $\bar{U}$ and U_0 are similar. As $\alpha^2 \to \alpha_c{}^2$ the Hartree-Fock values of $\bar{U}$ and U_0 depart from the Hartree values; $\bar{U}$ feels the effect of the Pauli principle more rapidly than U_0 and begins to go toward the Hartree-Fock liquid value. As $\alpha^2 \to 0$ both $\bar{U}$ and U_0 should be equal at the liquid value in a Hartree or Hartree-Fock calculation. An argument for the stronger effect of the Pauli principle on $\bar{U}$ is given in the text.

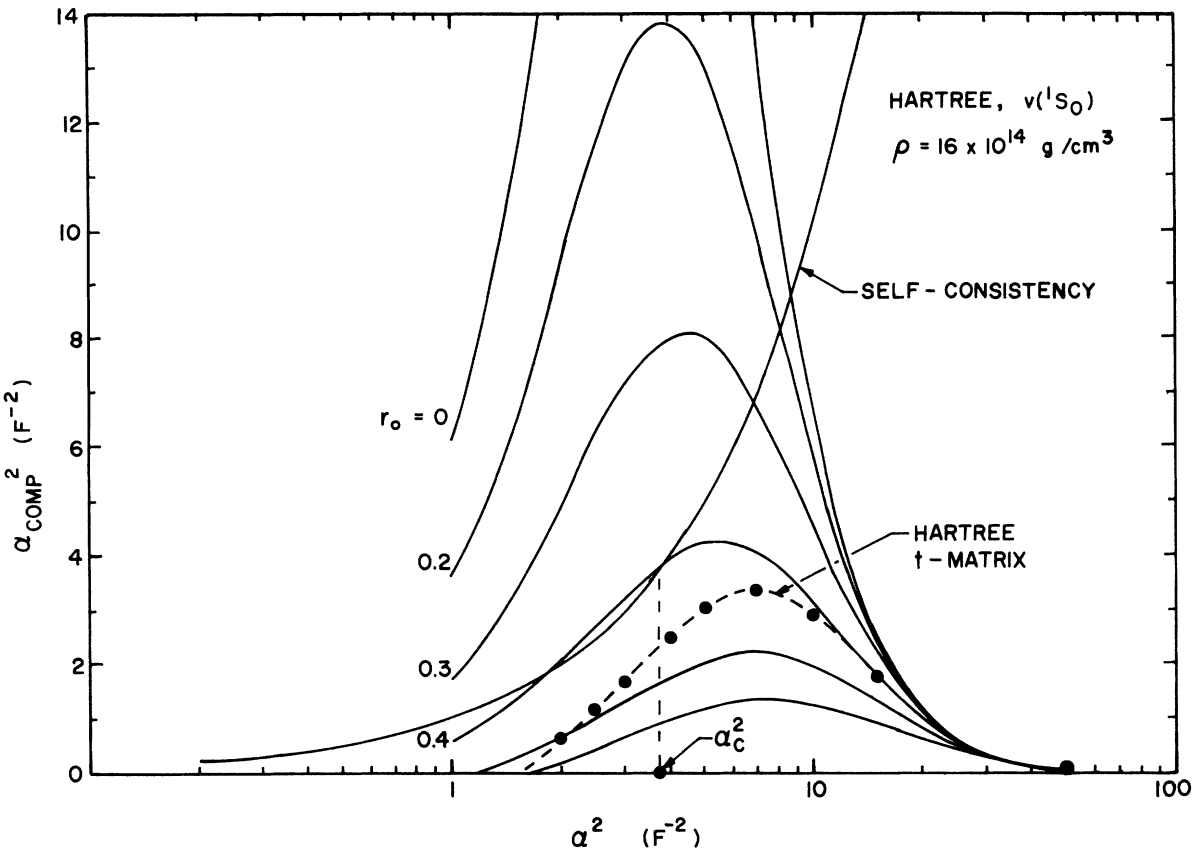

FIG. 8. The Hartree self-consistency condition for $v_{^1S_0}(r)$. We plot $\alpha_{\text{comp}}{}^2$ from Eq. (26) vs α^2 for the Hartree, correlated Hartree, and Hartree t-matrix cases. We show the result for the intermediate density, $\rho = 16\times 10^{14}$ g/cm^3. The results are quite similar to those in Figs. 1(a)–1(c) for the $v_R(r)$ potential. We note that the attractive part of the $^1S_0$ potential leads to a reduction of the effective repulsive core so that by $r_0 \approx 0.4$ the self-consistency condition is barely satisfied. There is no self-consistency for the Hartree t-matrix calculation.

used to evaluate U_0. In Fig. 13, however, the data in this region still remain reliable since $\overline{U}$ requires fewer partial waves for an accurate description. In Fig. 12 we note that our $\alpha_{\text{comp}}{}^2$ results using the full Reid soft-core potentials follow more closely the $\alpha_{\text{comp}}{}^2$ curve of the purely repulsive $v_R(r)$ than the attractive $v_{^1S_0}(r)$ potential. The most striking feature is the lack of self-consistency in the physical region in our computations for either the two model potentials or the full Reid soft-core potentials.[18] In Fig. 13 the energy-per-particle curve for the full Reid potential problem falls between the corresponding curves for the two model potentials. This is reasonable since the model potentials may be considered as envelope potentials for the complex set of Reid soft-core potentials. The potential $v_R(r)$ is purely repulsive while $v_{^1S_0}(r)$ is the most attractive of the Reid potentials. No energy minimum is observed except in the unphysical region for the $v_{^1S_0}(r)$ model potential. We observe qualitatively similar behavior in the two other densities that we have studied, 5×10^{14} and 50×10^{14} g/cm^3. In neither case do we obtain a self-consistency or an energy minimum except possibly in the unphysical region.

We have carried out our calculations only in the bcc phase. Since the tensor part of the nuclear interaction is dependent upon the spin configuration, one should examine the tensor force contribution for various spin and lattice configurations. However, as seen in Figs. 12 and 13 and explained in Appendix A, several different treatments of the tensor force contributions in a bcc lattice have produced similar results. This behavior is expected since the tensor force comprises only a small part of the interaction and also because, on the basis of our experience with the two model potentials, we do not expect minor modifications in the potential structure to significantly change our results. Thus, we have not examined crystallographic structures other than

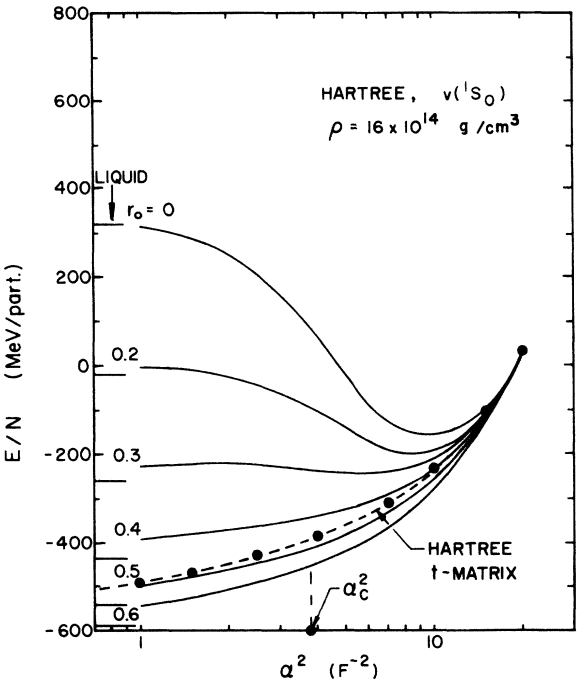

FIG. 9. The energy per particle in the Hartree approximations for $v_{^1S_0}(r)$. We show the energy per particle as a function of α^2 for $\rho = 16 \times 10^{14}$ g/cm^3 for the Hartree, correlated Hartree, and Hartree t-matrix calculations. For small α^2 the energy approaches the Hartree liquid energy.

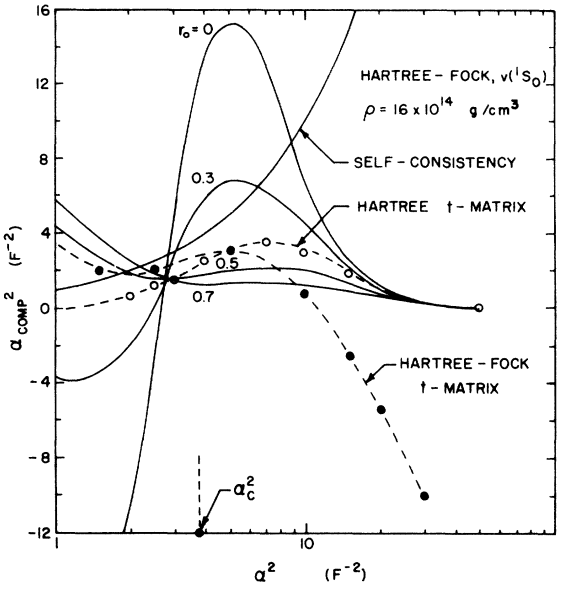

FIG. 10. The Hartree-Fock self-consistency condition for $v_{^1S_0}(r)$. We plot $\alpha_{\text{comp}}{}^2$ from Eq. (26) vs α^2 for the Hartree-Fock, correlated Hartree-Fock, and Hartree-Fock t-matrix cases. These results are for $\rho = 16 \times 10^{14}$ g/cm^3. At large α^2 the results are similar to the Hartree results. At small or nonphysical values of α^2 the results are unusual. We show the Hartree-Fock t-matrix and Hartree t-matrix for comparison and note that the Hartree-Fock t-matrix result departs below the Hartree result for large α^2. This is due to failure to include a sufficient number of partial waves. No self-consistency is achieved for the Hartree-Fock t-matrix.

the bcc lattice. It does not seem likely that a modification of the spin configuration would lead to a change in the tensor force contribution which would drastically alter our basic results.

There have been a number of earlier investigations of the solid-neutron-matter problem. The work we have presented here is most like that of Canuto and co-workers and our conclusions are most usefully related to theirs. We noted earlier that our solution to the $v_R(r)$ problem was similar to the result of Canuto, Chitre, and Lodenquai for the homework problem. The original calculation of Canuto and Chitre on the full solid-neutron-matter problem employed a formalism similar to the one we have employed here in the Hartree-Fock t-matrix approximation. However, because the pair Hamiltonian they used to find the t matrix was not parity conserving they were forced to deal with certain unnecessary complications. Their results differ markedly from any we have achieved. Although we are unable at present to undertake an exhaustive criticism of their work, some comment on our present understanding of their work may be instructive.

(1) The t matrix employed by Canuto and Chitre is found from the solution of a pair equation of motion in which a biased single-particle potential appears: viz.

$$U(\vec{r}) = \tfrac{1}{2} k(\vec{r} - \vec{\Delta})^2 . \tag{31}$$

This potential has the effect of not permitting a pair of particles to exchange place; i.e., it biases the relative coordinate wave function of the pair so that the region of relative coordinate space with $\vec{r} \approx \vec{\Delta}$ is much preferred to the region of relative coordinate space with $\vec{r} = -\vec{\Delta}$. The energy required to have $\vec{r} \approx -\vec{\Delta}$ is $2k\Delta^2 = (\hbar^2\alpha^2/m)\alpha^2\Delta^2 \approx 4000$ MeV for the solid states found by Canuto and Chitre. For the relative coordinate wave function to achieve the bias imposed by $U(\vec{r})$ it is necessary that it be constructed from unphysical states as well as physical states. By physical (unphysical) states, we refer to states with the correct (incorrect) spatial symmetry to properly antisymmetrize the total pair wave function. Since $U(\vec{r})$ is not symmetric (not parity conserving), the unphysical states must enter the analysis. For a parallel spin pair the physical states produce a spatially antisymmetric wave function of equal

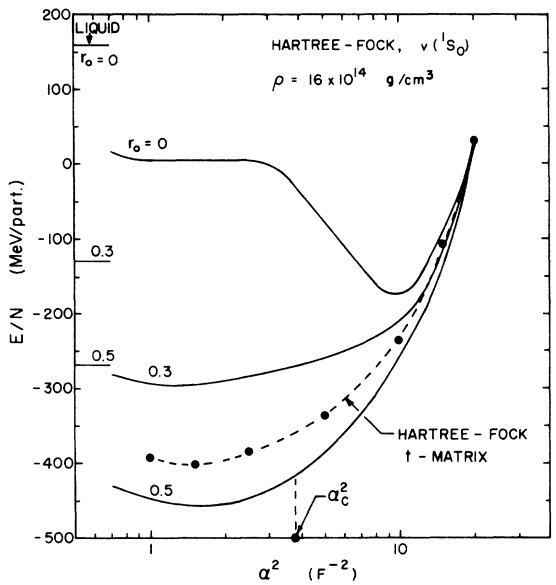

FIG. 11. The Hartree-Fock energy per particle for $v_{^1S_0}(r)$. We show the energy per particle as a function of α^2 for $v_{^1S_0}(r)$ in the Hartree-Fock, correlated Hartree-Fock, and Hartree-Fock t-matrix cases. The energies approach the corresponding liquid values as $\alpha^2 \to 0$. The energy per particle is not much different from the Hartree energy per particle.

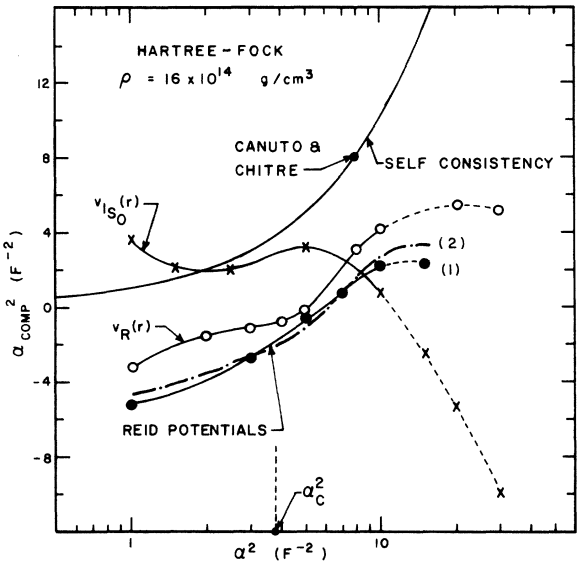

FIG. 12. The Hartree-Fock self-consistency condition for the Reid potentials. We plot α_{comp}^2 from Eq. (26) vs α^2 for the Hartree-Fock t-matrix case. We show the results for the two model potentials and the Reid soft-core potentials at $\rho = 16 \times 10^{14}$ g/cm^3. For the Reid soft-core potentials we show two curves that result from the several treatments of the spin quantization described in Appendix A. The curves labeled "(1)" and "(2)" correspond to methods (1) and (2) of Appendix A. We note that the various methods of treating the spin quantization produce little difference in the outcome of the calculations. We note that only the $v_{^1S_0}(r)$ problem satisfies the self-consistent condition (but in the nonplysical region). For $\alpha^2 > 10$ we dash the α_{comp}^2 curves to show that they are becoming less reliable as α^2 increases due to the limit on the number of partial waves we use. The location of the self-consistent α^2 found by Canuto and Chitre is shown.

but opposite amplitudes at $\vec{r} \approx \vec{\Delta}$ and $\vec{r} \approx -\vec{\Delta}$; the unphysical states produce a spatially symmetric wave function of equal amplitudes at $\vec{r} \approx \vec{\Delta}$ and $\vec{r} \approx -\vec{\Delta}$. In the total relative coordinate wave function the physical states and unphysical states add at $\vec{r} \approx -\vec{\Delta}$ to have zero (or very small) amplitude and the physical states and unphysical states add at $\vec{r} \approx \vec{\Delta}$ to have a large amplitude. If a pair of particles in the physical states has the same energy by virtue of their interaction with one another as a pair of particles in the unphysical states, then the interaction would tend to leave the amount of pair wave function in the physical and unphysical states unchanged; i.e., $|C_P|^2 \approx |C_{UP}|^2 \approx \frac{1}{2}$. If, on the other hand, a pair of particles in the physical state interacted with one another with a more attractive interaction than a pair of particles in the unphysical state, there would be a tendency to populate the physical state at the expense of the unphysical state. But this tendency would have to balance against the positive potential energy in $U(\vec{r})$ gained by having a finite wave function at $\vec{r} \approx -\vec{\Delta}$. This energy is of order $(\hbar^2\alpha^2/m)(\alpha^2\Delta^2)(|C_P|^2 - |C_{UP}|^2)$. The final relative coordinate wave function would represent a balance between these competing effects. The pair wave function found by Canuto and Chitre contains both physical and unphysical states. In calculating the potential energy for a pair of particles, Canuto and Chitre take only the physical part of the wave function. If the only effect of the competition between the physical and unphysical wave functions is to shift the amplitude of each while leaving the shape unchanged, the computational procedure of Canuto and Chitre should be quite satisfactory. But the equation of motion for the physical wave function is coupled to that for the unphysical wave function. A shift in the relative amplitudes of the physical and unphysical wave function is necessarily accompanied by a change in their shape. Thus the introduction of the unphysical wave function is not just a cumbersome artifact; it makes itself known through a distortion of the physical wave function. If this distortion is not large, the results of Canuto and Chitre should again be quite satisfactory. This argument does not apply for a problem involving state-independent potentials, i.e., it

does not apply to the work of Canuto, Chitre, and Lodenquai on the homework problem or on the helium problem, for in these problems particles in the physical and unphysical states have the same interaction with one another. On the other hand, for this reason the work on these state-independent problems does not demonstrate the adequacy of the formalism of Canuto and Chitre for the full neutron matter problem.

(2) We have a general expectation about the behavior of $\overline{U}$ and U_0 that is not met in the calculations of Canuto and Chitre. The quantity $\overline{U}$ is the average potential energy per particle in the presence of its neighbors when the relative motion of the particle with respect to its neighbors is described by $\exp[-(\alpha^2/2)(\vec{r}-\vec{\Delta})^2]$. The quantity U_0 is the potential energy of a particle on its lattice site. That is, U_0 is the average potential energy of a particle in the presence of its neighbors when the relative motion of the particle with respect to its neighbors is described by $\exp[-\alpha^2(\vec{r}-\vec{\Delta})^2]$. We expect

$$\overline{U}(2\alpha^2) \approx U_0(\alpha^2) . \tag{32}$$

This relation is borne out in our Hartree and Hartree-Fock calculations [see Figs. 7(a) and 7(b)]. This relationship does not seem to be correct for the calculations of Canuto and Chitre; e.g., see their Fig. 4.

(3) The calculation of U_0 by Canuto and Chitre seems to contain an error. When a particle is placed on its lattice site its relative motion with respect to its neighbors is described by a combination of the relative-coordinate wave function *and* the center-of-mass wave function. Thus, if there is a state-dependent interaction it is not proper to move the center-of-mass part of this relative motion through the interaction. This is most easily seen by writing

$$\int d\vec{x}_i \int d\vec{x}_j \Phi(ij) v(ij) \psi(ij) \delta(\vec{x}_i - \vec{R}_i)$$

in the form

$$\int d\vec{R} \int d\vec{r}\, \Phi(\vec{R}) \phi(\vec{r}) v(\vec{r}) \Phi(\vec{R}) \psi(\vec{r})\, \delta(\vec{R} - \vec{d} - \tfrac{1}{2}\vec{r} + \tfrac{1}{2}\vec{\Delta}) .$$

We complete this section by commenting briefly on the work on the "homework" problem by Chakravarty, Miller, and Woo. The most striking feature of the state which they obtain is that the "number of particles per particle" as measured by n is of order 10–20 (see Fig. 4). This state is certainly not a solid. For example, it has almost an order of magnitude less energy of localization at a given density than a Fermi gas

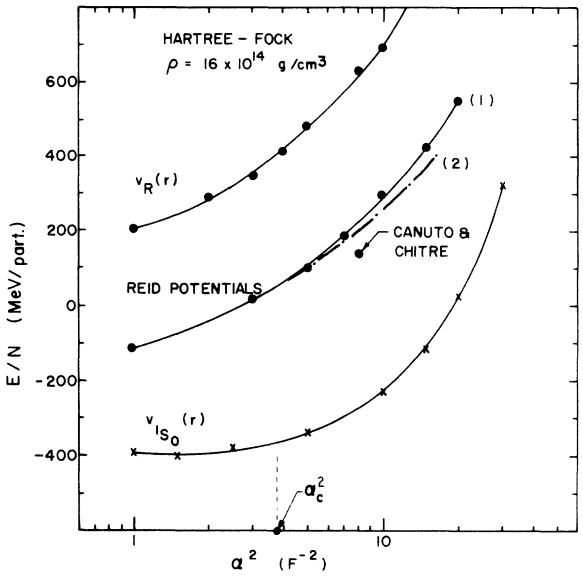

FIG. 13. The energy per particle in the Hartree-Fock approximation with the Reid potentials. We show the energy per particle as a function of α^2 for $\rho = 16\times 10^{14}$ g/cm^3 for the two model potentials and the Reid soft-core potentials. For the Reid soft-core potentials we show two curves that result from the several treatments of the spin quantization described in Appendix A. The curves labeled "(1)" and "(2)" correspond to methods (1) and (2) of Appendix A. We note that the various methods of treating the spin quantization produces little difference in the outcome of the calculations. The energy per particle for the Reid soft-core potentials is midway between the results for the most repulsive case, $v_R(r)$, and the most attractive case, $v_{^1S_0}(r)$. We show the energy found by Canuto and Chitre at this density. The similarity of their energy to ours suggests that the disagreement between the two calculations has to do with the self-consistency condition.

at that density. In fact, this state should be an excellent approximation to a liquid. Thus the solid energies found by Chakravarty, Miller, and Woo should be essentially the same as those they found for the liquid. The fact that they find $E_S/E_L \approx \frac{2}{3}$ is very puzzling. We find $E_S/E_L \approx 1$ at $\alpha^2 \gtrsim 1$ for reasonable potentials.

V. CONCLUSION

We have studied the solid-neutron-matter problem in a sequence of approximations: Hartree, Hartree t matrix, Hartree-Fock, and Hartree-Fock t matrix. We have applied these approximations extensively to two simplified problems: neutrons interacting with the repulsive part of the $^1S_0$ potential and with the full $^1S_0$ potential. We have carefully discussed the results of our calculations for the two model problems in order to

establish the adequacy of our treatment in each of the approximations we use. For the Hartree and Hartree-Fock approximations we find self-consistent solutions for a solid state. For the Hartree t-matrix and Hartree-Fock t-matrix approximations we find no self-consistent solutions or unphysical self-consistent solutions for the solid state. These results are in reasonable agreement[19] with those of Østgaard[18] and Canuto, Chitre, and Lodenquai.[9] The formalism we have developed for the Hartree-Fock t-matrix approximation is able to incorporate all of the features found in the neutron matter problem when the neutrons interact through the Reid soft-core potentials. When this formalism is applied to this problem we find no self-consistent solutions for the solid state. Therefore we conclude that Reid soft-core neutrons have no solid state.

ACKNOWLEDGMENT

We would like to thank Professor James F. Walker for very valuable comments on several aspects of this problem.

APPENDIX A

In this appendix we exhibit the detailed equations that are employed in the calculation of $\overline{U}$ and U_0 in the Hartree-Fock t-matrix approximation. Special considerations must be made to antisymmetrize properly the pair wave functions and to account for the external spin quantization axis.

For $\overline{U}$, the average value of the potential experienced by particle i, we have

$$\overline{U} = \sum_{j \neq (i)} \left[\overline{U}_{\uparrow\downarrow}(ij)\delta_{\uparrow\downarrow,ij} + \overline{U}_{\uparrow\uparrow}(ij)\delta_{\uparrow\uparrow,ij} \right] . \tag{A1}$$

We note that the index i is suppressed in $\overline{U}$ and U_0 since these quantities are independent of i. We examine both terms in this sum separately. First, we have

$$\overline{U}_{\uparrow\downarrow}(ij) = \frac{\int d\vec{\mathbf{x}}_i \int d\vec{\mathbf{x}}_j [\phi^+(ij)\overline{X}_{00} + \phi^-(ij)\overline{X}_{10}] v(ij) [\psi^+(ij)\overline{X}_{00} + \psi^-(ij)\overline{X}_{10}]}{\int d\vec{\mathbf{x}}_i \int d\vec{\mathbf{x}}_j [\phi^+(ij)\overline{X}_{00} + \phi^-(ij)\overline{X}_{10}] [\psi^+(ij)\overline{X}_{00} + \psi^-(ij)\overline{X}_{10}]} , \tag{A2}$$

where $\phi^{\pm}(ij) = \phi(\vec{\mathbf{R}})\phi^{\pm}(\vec{\mathbf{r}})$, $\psi^{\pm}(ij) = \phi(\vec{\mathbf{R}})\psi^{\pm}(\vec{\mathbf{r}})$,

$$\phi^{\pm}(\vec{\mathbf{r}}) = \sum_{\substack{L=0,2,4,\ldots \\ L=1,3,5,\ldots}} R_L^{\pm}(r) Y_{L0}(\Omega) , \tag{A3}$$

$$\psi^{\pm}(\vec{\mathbf{r}}) = \sum_{\substack{L=0,2,4,\ldots \\ L=1,3,5,\ldots}} g_L^{\pm}(r) R_L^{\pm}(r) Y_{L0}(\Omega) , \tag{A4}$$

and $\overline{X}_{SM_S}$ are the total spin wave functions for a pair of spin-$\frac{1}{2}$ neutrons. The spin axis of quantization is chosen along some arbitrary external direction. The Reid potentials are defined in terms of matrix elements for pairs of particles described by J and S, i.e.,

$$v_{LL'}^{JS}(r) = \langle r; JM_J, LS | v | r; J'M_{J'}, L'S' \rangle \times \delta_{JJ'}\delta_{M_J M_{J'}}\delta_{SS'}\delta_{L,(L' \text{ or } L'\pm 2)} . \tag{A5}$$

For $J > 2$, we used the approximations of Canuto and Chitre: $v_{22}^{20}(r) = v(^1D_2)$ for even L and the central part of $v_{11}^{21}(r) = v_c(^3P_2 - {}^3F_2)$ for odd L.

Proper antisymmetrization of the pair wave function requires that even L be coupled to $S=0$ and odd L to $S=1$. Thus, we can write

$$\overline{U}_{\uparrow\downarrow}(ij) = \frac{\overline{U}_{\uparrow\downarrow}^{(+0)}(ij) + \overline{U}_{\uparrow\downarrow}^{(-1)}(ij)}{N_{\uparrow\downarrow}^{+}(ij) + N_{\uparrow\downarrow}^{-}(ij)} , \tag{A6}$$

where the $(+, -)$ and $(0, 1)$ superscripts on the $\overline{U}_{\uparrow\downarrow}(ij)$ refer to the parity of the partial waves involved and the total spin S of the pair, respectively. The normalization terms in the denominator are

$$N_{\uparrow\downarrow}^{\pm}(ij) = \int_0^{+\infty} r^2 dr \sum_{\substack{L=0,2,\ldots \\ L=1,3,\ldots}} |R_L^{\pm}(r)|^2 g_L^{\pm}(r) . \tag{A7}$$

The even-L, $S=0$ contribution to $\overline{U}_{\uparrow\downarrow}(ij)$ can be expanded as

$$\overline{U}_{\uparrow\downarrow}^{(+0)}(ij) = \int_0^{+\infty} r^2 dr \sum_{L=0,2,\ldots} |R_L^{+}(r)|^2 g_L^{+}(r) v_{LL}^{L0}(r) . \tag{A8}$$

When we examine the odd-L, $S=1$ contribution to $\overline{U}_{\uparrow\downarrow}(ij)$, however, we must rotate the spin quantization axis, which has some fixed external direction, to lie along the axis of quantization of $\vec{\mathbf{L}}$, which is chosen to be along $\vec{\Delta}_{ij}$, the direction pointing from lattice site i to lattice site j (see Pandharipande, Ref. 5). Thus, if $\overline{X}_{1\bar{m}_s}$ is a spin

state relative to the external quantization axis, then

$$\bar{X}_{1\bar{m}_s} = \sum_{m_s=-1,0,1} D_{\bar{m}_s m_s}(\beta_{ij}) X_{1m_s} \ , \tag{A9}$$

where the X_{1m_s} are spin-1 states relative to a spin quantization axis parallel to the quantization axis for $\vec{L}$, β_{ij} is the angle between the external $\vec{S}$ axis and the $\vec{L}$ axis of quantization, and $D_{\bar{m}_s m_s}(\beta_{ij})$ are the elements of the rotation matrix about an angle β_{ij}. The rotation matrix is

$$D(\beta) = \begin{bmatrix} \cos^2(\frac{1}{2}\beta) & -\frac{1}{\sqrt{2}}\sin\beta & \sin^2(\frac{1}{2}\beta) \\ \frac{1}{\sqrt{2}}\sin\beta & \cos\beta & -\frac{1}{\sqrt{2}}\sin\beta \\ \sin^2(\frac{1}{2}\beta) & \frac{1}{\sqrt{2}}\sin\beta & \cos^2(\frac{1}{2}\beta) \end{bmatrix} \tag{A10}$$

The odd-L, $S=1$ contribution can now be written as

$$\bar{U}^{(-1)}_{\uparrow\uparrow}(ij) = \int_0^{+\infty} r^2 dr \sum_j \sum_{\substack{L=1,3,\dots \\ L'=1,3,\dots}} \left[\sum_{m_s=-1,0,1} |D_{\bar{m}_s m_s}(\beta_{ij})|^2 C^{L\,1\,J}_{0m_s m_s} C^{L'\,1\,J}_{0m_s m_s} \right] R^-_L(r) R^-_{L'}(r) g^-_L(r) v^{J\,1}_{LL'}(r), \tag{A11}$$

where $\bar{m}_s = 0$ since we are considering an $\uparrow\uparrow$ pair. The term in square brackets (sum over m_s) deserves special attention. We have examined it in three different ways.

(1) We choose $\beta_{ij} = 0$ for all pairs, i.e., the axes of quantization for $\vec{S}$ and $\vec{L}$ were chosen to be along the same direction for each pair in the sum in Eq. (A1). Thus,

$$\bar{U}^{(-1)}_{\uparrow\uparrow}(ij) = \int_0^{+\infty} r^2 dr \sum_J \sum_{\substack{L=1,3,\dots \\ L'=1,3,\dots}} C^{L\,1\,J}_{000} C^{L'\,1\,J}_{000} R^-_L(r) R^-_{L'}(r) \times g^-_L(r) v^{J\,1}_{LL'}(r) . \tag{A12}$$

(2) We calculate the angular average over each shell. A shell corresponds to those particles which are equidistant from particle i. Thus, since

$$\frac{1}{4\pi} \int d\Omega \, |D_{\bar{m}_s m_s}(\beta)|^2 = \tfrac{1}{3} \text{ for all } \bar{m}_s \text{ and } m_s ,$$

where $d\Omega = \sin\beta \, d\beta \, d\phi$, and since it can be shown that

$$\frac{1}{3} \sum_{m_s=-1,0,1} C^{L\,1\,J}_{0m_s m_s} C^{L'\,1\,J}_{0m_s m_s} = \frac{1}{3}\left(\frac{2J+1}{2L+1}\right)\delta_{LL'} , \tag{A13}$$

then

$$\bar{U}^{(-1)}_{\uparrow\uparrow}(ij) = \int_0^{+\infty} r^2 dr \sum_J \sum_{L=1,3,\dots} \frac{1}{3}\left(\frac{2J+1}{2L+1}\right) |R^-_L(r)|^2 \times g^-_L(r) v^{J1}_{LL}(r) . \tag{A14}$$

This angular-averaging procedure distributes the particles, located at discrete points on a shell, uniformly over the shell. For a shell with a large number of particles this procedure must be a good approximation. But, it is even better than that; see below.

(3) We treat the sum over m_s exactly. This exact treatment, however, produces results nearly identical to those of method (2) where we calculated the angular average. This can be shown by a detailed examination of the terms of the summation over m_s. First, we note that

$$C^{L\,1\,J}_{0-1-1} C^{L'\,1\,J}_{0-1-1} = (-1)^{L+1-J} C^{L\,1\,J}_{011} (-1)^{L'+1-J} C^{L'\,1\,J}_{011} = C^{L\,1\,J}_{011} C^{L'\,1\,J}_{011} . \tag{A15}$$

The last equality holds since we are considering only odd L and L'. Thus the sum over m_s may be expanded to yield

$$\sum_{m_s=-1,0,1} |D_{m_s}|^2 C^{L\,1\,J}_{0m_s m_s} C^{L'\,1\,J}_{0m_s m_s} = [\,|D_1|^2 + |D_{-1}|^2\,] C^{L\,1\,J}_{011} C^{L'\,1\,J}_{011} + |D_0|^2 C^{L\,1\,J}_{000} C^{L'\,1\,J}_{000} , \tag{A16}$$

where

$$D_{m_s} \equiv D_{\bar{m}_s m_s}(\beta_{ij}) , \tag{A17}$$

and for convenience we have suppressed the $\bar{m}_s$ and β_{ij} dependence in writing D_{m_s}. We must evaluate this sum [Eq. (A16)] for all allowed combinations of (L, L', J). Table I shows the results for L and L' equal to 1 or 3 after the relevant Clebsch-Gordan coefficients have been evaluated. [For all odd $L \geq 5$, a purely central potential is used—see immediately after Eq. (A5) whence a

TABLE I. Contribution of various (L, L', J) terms to the sum over m_s of Eq. (A16) and the angular-averaged results, $\frac{1}{3}[(2J+1)/(2L+1)]\delta_{LL'}$, of Eq. (A13).

(L, L', J)	Method (3) $\sum_{m_s} \lvert D_{m_s}\rvert^2 C^{L1J}_{0m_s m_s} C^{L'1J}_{0m_s m_s}$	Method (2) Angular averaging
(1, 1, 0)	$\frac{1}{3}\lvert D_0\rvert^2$	$\frac{1}{9}$
(1, 1, 1)	$\frac{1}{2}(\lvert D_1\rvert^2+\lvert D_{-1}\rvert^2)$	$\frac{3}{9}$
(1, 1, 2)	$\frac{1}{2}(\lvert D_1\rvert^2+\lvert D_{-1}\rvert^2)+\frac{2}{3}\lvert D_0\rvert^2$	$\frac{5}{9}$
(1, 3, 2) } (3, 1, 2) }	$(1/\sqrt{14})(\lvert D_1\rvert^2+\lvert D_{-1}\rvert^2)-(2/\sqrt{14})\lvert D_0\rvert^2$	0
(3, 3, 2)	$\frac{1}{7}(\lvert D_1\rvert^2+\lvert D_{-1}\rvert^2)+\frac{3}{7}\lvert D_0\rvert^2$	$\frac{5}{21}$
(3, 3, 3)	$\frac{1}{2}(\lvert D_1\rvert^2+\lvert D_{-1}\rvert^2)$	$\frac{7}{21}$
(3, 3, 4)	$\frac{5}{14}(\lvert D_1\rvert^2+\lvert D_{-1}\rvert^2)+\frac{4}{7}\lvert D_0\rvert^2$	$\frac{9}{21}$

simplified form like Eq. (A8) results:

$$\bar{U}^{(-1)}_{\uparrow\downarrow}(ij)\big|_{L\geq 5} = \int_0^{+\infty} r^2 dr \sum_{L=5,7,\ldots} \lvert R^-_L(r)\rvert^2 g^-_L(r) \times v_c({}^3P_2 - {}^3F_2)\,. \tag{A18}$$

Thus, we need to only concern ourseives with the noncentral $L \leq 3$ terms.] The angular-averaged results which are also presented in Table I are those obtained in method (2) by assuming a uniform particle density for a given shell. For the present case where the particles are treated as discrete particles on lattice sites, we must evaluate $\lvert D_0\rvert^2$ and $[\lvert D_1\rvert^2+\lvert D_{-1}\rvert^2]$ for each particle of a given shell. We note that the sum over m_s would be identically equal to the angular-averaged results of method (2) if

$$\lvert D_0\rvert^2 = \lvert D_{\bar{m}_s 0}(\beta_{ij})\rvert^2 = \tfrac{1}{3} \tag{A19}$$

and

$$\lvert D_1\rvert^2+\lvert D_{-1}\rvert^2 = \lvert D_{\bar{m}_s 1}(\beta_{ij})\rvert^2+\lvert D_{\bar{m}_s -1}(\beta_{ij})\rvert^2 = \tfrac{2}{3}\,. \tag{A20}$$

This, of course, does not hold for each pair of particles i and j. However, if we take the average value of $\lvert D_0\rvert^2$ and $[\lvert D_1\rvert^2+\lvert D_{-1}\rvert^2]$ over all the particles of a given shell, then this result holds exactly. The proof of this is given in Appendix D. Note that this is a discrete average over all of the particles of a given shell and not an angular average over a uniform particle density as in method (2).

Averaging over all of the particles in a shell is not, however, entirely legitimate since the correlation function $g^-_L(r)$ differs for different pairs in the same shell. This difference reflects the changing amounts of the $v^J_{LL'}(r)$ that interact as β_{ij} varies. This difference produces small corrections, however, since the partial waves $R^-_L(r)$ already possess strong correlations due to the large angular momentum repulsive barrier (for $L \geq 1$). The $g_L(r)$ produce small corrections (for $L \geq 1$) in the calculation of U_0 and $\bar{U}$. Therefore to good approximation, method (3) is identical to method (2).

In the main body of this paper we have presented the results using methods (1) and (2) when appropriate, that is, when we use the full set of state- and spin-dependent potentials (see Figs. 12 and 13). We note that an insubstantial change in all features of the calculation results when method (2) or (3) of treating the spin quantization is used in place of method (1).

The second term in Eq. A1 can be treated similarly to the first term. We have

$$\bar{U}_{\uparrow\uparrow}(ij) = \frac{\int d\vec{\mathbf{x}}_i \int d\vec{\mathbf{x}}_j [\phi^-(ij)\bar{X}_{11}] v_{ij} [\psi^-(ij)\bar{X}_{11}]}{\int d\vec{\mathbf{x}}_i \int d\vec{\mathbf{x}}_j [\phi^-(ij)\bar{X}_{11}][\psi^-(ij)\bar{X}_{11}]} \tag{A21}$$

or

$$\bar{U}_{\uparrow\uparrow}(ij) = \frac{\bar{U}^{(-)}_{\uparrow\uparrow}(ij)}{N_{\uparrow\uparrow}(ij)}\,, \tag{A22}$$

where $\bar{U}^{(-1)}_{\uparrow\uparrow}(ij)$ is given by Eq. (A11) with $\bar{m}_s = 1$. We again handle the summation over m_s using methods (1) and (2) as we discussed earlier. The normalization term is similar to Eq. (A7) with only the odd L's taken in the sum. For U_0 we have

$$U_0 = \sum_{j\neq(i)} [U_{0\uparrow\uparrow}(ij)\delta_{\uparrow\uparrow,ij} + U_{0\uparrow\uparrow}(ij)\delta_{\uparrow\uparrow,ij}]\,, \tag{A23}$$

where

$$U_{0\uparrow\downarrow}(ij)=\left(\frac{\alpha^2}{\pi}\right)^{-3/2}\frac{\int d\vec{x}_i\int d\vec{x}_j[\phi^+(ij)\bar{X}_{00}+\phi^-(ij)\bar{X}_{10}]\,v(ij)[\psi^+(ij)\bar{X}_{00}+\psi^-(ij)\bar{X}_{10}][\delta(\vec{x}_i-\vec{R}_i)+\delta(\vec{x}_j-\vec{R}_j)]}{\int d\vec{x}_i\int d\vec{x}_j[\phi^+(ij)\bar{X}_{00}+\phi^-(ij)\bar{X}_{10}][\psi^+(ij)\bar{X}_{00}+\psi^-(ij)\bar{X}_{10}]}\,. \tag{A24}$$

Using $\phi^\pm(ij)=\phi(R)\phi^\pm(r)$, $\psi^\pm(ij)=\phi(\vec{R})\psi^\pm(\vec{r})$ and the δ functions in the form

$$\delta(\vec{x}_i-\vec{R}_i)+\delta(\vec{x}_i-\vec{R}_j)=\delta(\vec{R}-\vec{d}-\tfrac{1}{2}(\vec{r}-\vec{\Delta}))+\delta(\vec{R}-\vec{d}-\tfrac{1}{2}(\vec{r}+\vec{\Delta})) \tag{A25}$$

we have

$$\phi(\vec{R})[\delta(\vec{x}_i-\vec{R}_i)+\delta(\vec{x}_i-\vec{R}_j)]=4\phi^+(\vec{r})\,. \tag{A26}$$

Thus we can write Eq. (A24) in the form

$$U_{0\uparrow\downarrow}(ij)=16\left(\frac{\alpha^2}{\pi}\right)^{-3/2}\frac{\int d\vec{r}\,\phi^+(\vec{r})[\phi^+(\vec{r})\bar{X}_{00}+\phi^-(\vec{r})\bar{X}_{10}]\,v(r)[\psi^+(\vec{r})\bar{X}_{00}+\psi^-(\vec{r})\bar{X}_{10}]\,\phi^+(\vec{r})}{\int d\vec{r}[\phi^+(\vec{r})\bar{X}_{00}+\phi^-(\vec{r})\bar{X}_{10}][\psi^+(\vec{r})\bar{X}_{00}+\psi^-(\vec{r})\bar{X}_{10}]}+\text{an overlap term}\,. \tag{A27}$$

The overlap term contains $\phi^+(\vec{r})+\phi^-(\vec{r})$ and $\phi^+(\vec{r})-\phi^-(\vec{r})$ in place of the two $\phi^+(\vec{r})$ produced by the center-of-mass wave function. In the physical region this overlap is small and can be neglected. Now to use the Reid potentials we need to find the partial-wave decomposition of the relative motion described by $\phi^+\phi^+$, $\phi^+\phi^-$ and $\phi^+\psi^+$, $\phi^+\psi^-$ on the left and right of $v(r)$, respectively. We define

$$B_L^\pm(r)=\sum_{L'=0,2,\ldots}\ \sum_{\substack{L''=0,2,\ldots\\ L''=1,3,\ldots}}\left[\frac{(2L'+1)(2L''+1)}{4\pi(2L+1)}\right]^{1/2}\times(C_{000}^{L'L''L})^2R_{L'}^+(r)R_{L''}^\pm(r) \tag{A28}$$

Similar to Eq. (A6) for $\bar{U}_{\uparrow\downarrow}(ij)$, we can now write

$$U_{0\uparrow\downarrow}(ij)=\frac{U_{0\uparrow\downarrow}^{(+0)}(ij)+U_{0\uparrow\downarrow}^{(-1)}(ij)}{N_{\uparrow\downarrow}^+(ij)+N_{\uparrow\downarrow}^-(ij)}\,. \tag{A29}$$

The normalization terms $N_{\uparrow\downarrow}^\pm(ij)$ are those given by Eq. (A7). The $U_{0\uparrow\downarrow}(ij)$ terms are similar to the corresponding $\bar{U}_{\uparrow\downarrow}(ij)$ terms given in Eqs. (A8), (A11), (A12), and (A14) except that all the $R_L^\pm(r)$ terms are replaced with their corresponding $B_L^\pm(r)$ terms defined above.

Finally, $U_{0\uparrow\uparrow}(ij)$ is handled in the same manner as $\bar{U}_{\uparrow\uparrow}(ij)$. Thus

$$U_{0\uparrow\uparrow}(ij)=\frac{U_{0\uparrow\uparrow}^{(-1)}(ij)}{N_{\uparrow\uparrow}^-(ij)}\,, \tag{A30}$$

where the normalization term is the same as that used in Eq. (A22) and $U_{0\uparrow\uparrow}^{(-1)}(ij)$ is given by Eq. (A11) with $\bar{m}_s=1$ and with all the $R_L^-(r)$ replaced with their corresponding $B_L^-(r)$.

In our numerical computations involving the partial-wave sums described in this appendix, we used 10 partial waves, $L=0, 2, 4, 6, 8$ for the even sums and $L=1, 3, 5, 7, 9$ for the odd sums.

APPENDIX B

In this appendix we discuss a few of the important features of the partial-wave decomposition of the relative-coordinate wave function. A pair of particles separated by distance $\vec{\Delta}$ have their relative motion described by

$$\Phi^\pm(\vec{r})=\frac{\theta_R(\vec{r})\pm\theta_L(\vec{r})}{\sqrt{2}}\,, \tag{B1}$$

where

$$\theta_{L,R}(\vec{r})=\left(\frac{\alpha^2}{2\pi}\right)^{3/4}\exp\left[-\frac{\alpha^2}{4}(\vec{r}\pm\vec{\Delta})^2\right]\,. \tag{B2}$$

For this relative-coordinate wave function we have (following a lengthy but straightforward calculation)

$$\langle\vec{L}^2\rangle=\frac{\hbar^2\alpha^2\Delta^2}{2}\,. \tag{B3}$$

In achieving this result we have assumed that the pair of particles are far enough apart that an overlap contribution to $\langle\vec{L}^2\rangle$ is negligible. This result can be understood by the argument

$$\langle\Delta r^2\rangle\langle\Delta p^2\rangle\approx\hbar^2\,,$$

where $\langle\Delta r^2\rangle$ is a measure of the size of the relative-coordinate wave function and $\langle\Delta p^2\rangle$ is the momentum perpendicular to $\vec{\Delta}$. Since $\langle\Delta r^2\rangle \approx 2/\alpha^2$ and $\langle L^2\rangle\approx(p\Delta)^2$ we have

$$\langle\vec{L}^2\rangle\approx\frac{\hbar^2\alpha^2\Delta^2}{2}\,, \tag{B4}$$

in agreement with Eq. (B3). If we write Eq. (B3) in the form $\langle L^2\rangle=\hbar^2l(l+1)$ we have a measure of the average angular momentum associated with the relative motion; i.e.,

$$l(l+1)=\frac{\alpha^2\Delta^2}{2}\,. \tag{B5}$$

As a pair of particles are further away from one another, Δ increases and the angular momentum decomposition of the relative-coordinate wave function involves more partial waves. As the relative motion becomes more localized α^2 becomes larger, the momentum uncertainty becomes larger, and so does $\bar{l}$. This result places a practical limit on the accuracy of a partial-wave description of the relative motion (see for example the comment in the text about the large-α^2 behavior of the Hartree-Fock calculations in Fig. 5). If the range of the interaction is well defined, we must consider pairs of particles only within a certain distance of one another. If the range of the interaction is b, then $\bar{l}$ for the important pairs of particles is about

$$\bar{l} \approx \alpha b . \tag{B6}$$

For the nuclear problem $b \lesssim 1$ F so that $l \approx \alpha$. This number is of order 5 for the worst case. Retaining partial waves with l much greater than 5 should produce no dramatic changes.

The angular momentum can also be calculated from

$$\langle \vec{L}^2 \rangle = \hbar^2 \bar{l}(\bar{l}+1) = \sum_{l=0}^{+\infty} |c_l|^2 l(l+1), \tag{B7}$$

where $|c_l|^2$ is a measure of how much of a given partial wave is in the realtive-coordinate wave function. It is again straightforward but tedious to calculate $|c_l|^2$ for $\phi^{\pm}(\vec{r})$ of Eq. (B1). We obtain the results shown in Table II. In all cases, $\sum |c_l|^2 l(l+1)$ agrees with the results of Eq. (B3) to within 1%. We note that although $\frac{1}{2}\alpha^2\Delta^2$ changes by a factor of 4 and $\bar{l}$ by a factor of about 2, the amplitudes $|c_l|^2$ remain largest for relatively small values of l. For $\frac{1}{2}\alpha^2\Delta^2 = 20$ and $\bar{l} \approx \sqrt{20} \approx 4.5$, well over 60% of the amplitude is in the $l=2$ and $l=4$ partial waves.

TABLE II. $|c_l|^2$ for even and odd partial waves for four different values of $\frac{1}{2}\alpha^2\Delta^2$. $|c_l|^2$ is a measure of how much of a given partial wave is in the relative-coordinate wave function $\phi^{\pm}(\vec{r})$. In terms of the partial-wave decomposition given by Eq. (A3), $|c_l|^2 = \int_0^\infty r^2 dr |R_L^{\pm}(r)|^2$.

	$\frac{\alpha^2\Delta^2}{2}=5$			$\frac{\alpha^2\Delta^2}{2}=10$			$\frac{\alpha^2\Delta^2}{2}=15$			$\frac{\alpha^2\Delta^2}{2}=20$		
l	$\lvert C_l\rvert^2$	l	$\lvert C_l\rvert^2$	l	$\lvert C_l\rvert^2$	l	$\lvert C_l\rvert^2$	l	$\lvert C_l\rvert^2$	l	$\lvert C_l\rvert^2$	l	$\lvert C_l\rvert^2$
0	0.2802	1	0.6141	0	0.1700	1	0.4239	0	0.1200	1	0.3169	0	0.0925	1	0.2518
2	0.5286	3	0.2662	2	0.4880	3	0.3923	2	0.4094	3	0.3914	2	0.3458	3	0.3622
4	0.0873	5	0.0197	4	0.2411	5	0.1176	4	0.3030	5	0.1968	4	0.3165	5	0.2390
6	0.0033	7	0.0003	6	0.0465	7	0.0152	6	0.1093	7	0.0525	6	0.1587	7	0.0937
				8	0.0041	9	0.0009	8	0.0220	9	0.0081	8	0.0496	9	0.0236
				10	0.0019	11	0.0000	10	0.0026	11	0.0007	10	0.0101	11	0.0039
								12	0.0002	13	0.0000	12	0.0014	13	0.0004
												14	0.0001	15	0.0000
	$\sum \lvert C_l\rvert^2 = 0.8995$			$\sum \lvert C_l\rvert^2 = 0.9500$			$\sum \lvert C_l\rvert^2 = 0.9666$			$\sum \lvert C_l\rvert^2 = 0.9750$		
	$\langle L^2 \rangle = 5.057$			$\langle L^2 \rangle = 10.02$			$\langle L^2 \rangle = 15.014$			$\langle L^2 \rangle = 20.009$		

APPENDIX C

Consider

$$\psi_{\uparrow\downarrow} = A\Phi^+ X_{00} + B\Phi^- X_{10}, \tag{C1}$$

where

$$\Phi^+(\vec{r}) = \sum_{L \in \mathbb{E}} R_L^+(r) Y_{L0}(\Omega), \tag{C2}$$

$$\Phi^-(\vec{r}) = \sum_{L \in \mathbb{O}} R_L^-(r) Y_{L0}(\Omega), \tag{C3}$$

and

$$X_{00} = \frac{\alpha(1)\beta(2) - \beta(1)\alpha(2)}{\sqrt{2}}, \tag{C4}$$

$$X_{10} = \frac{\alpha(1)\beta(2) + \beta(1)\alpha(2)}{\sqrt{2}}, \tag{C5}$$

where $\alpha(1)$ and $\beta(1)$ are the spin-$\frac{1}{2}$ wave functions for particle 1. In the summation, $L \in \mathrm{E}$ and $L \in \mathrm{O}$ restrict the sums to even or odd L. We take $\Phi^+(\vec{r})$ and $\Phi^-(\vec{r})$ to be separately normalized to 1. Since

$$\int d\Omega\, Y_{L0}(\Omega) Y_{L'0}(\Omega) = \delta_{LL'}, \tag{C6}$$

this means

$$\sum_{L\in \mathrm{E}} \int_0^{+\infty} |R_L^+(r)|^2 r^2 dr = 1 \tag{C7}$$

and

$$\sum_{L\in \mathrm{O}} \int_0^{+\infty} |R_L^-(r)|^2 r^2 dr = 1 . \tag{C8}$$

Thus

$$\langle \psi_{\uparrow\downarrow} | \psi_{\uparrow\downarrow} \rangle = (|A|^2 + |B|^2) = 1 .$$

If we want to attach a particular *spin* to a particular lattice site, as we do in considering a lattice with a particular spin arrangement, then from Eqs. (C1)–(C5) we have

$$\psi_{\uparrow\downarrow} = \left[A \sum_{L\in \mathrm{E}} R_L^+(r) Y_{L0}(\Omega) + B \sum_{L\in \mathrm{O}} R_L^-(r) Y_{L0}(\Omega)\right] \frac{\alpha(1)\beta(2)}{\sqrt{2}}$$

$$- \left[A \sum_{L\in \mathrm{E}} R_L^+(r) Y_{L0}(\Omega) - B \sum_{L\in \mathrm{O}} R_L^-(r) Y_{L0}(\Omega)\right] \frac{\beta(1)\alpha(2)}{\sqrt{2}} . \tag{C9}$$

To have a particular spin associated with a particular site requires (1) that when $\vec{r}$ points toward $\vec{\Delta} = \vec{R}_i - \vec{R}_j$ the coefficient of $\alpha(1)\beta(2)$ is nonzero and the coefficient of $\beta(1)\alpha(2)$ is zero, and (2) that when $\vec{r}$ points toward $-\vec{\Delta} = (\vec{R}_i - \vec{R}_j)$ the coefficient of $\alpha(1)\beta(2)$ is zero and the coefficient of $\beta(1)\alpha(2)$ is nonzero. In the absence of specific formulas for the $R_L(r)$ we must argue qualitatively. Assuming the even and odd $R_L(r)$ to be approximately equal we have $A \approx B \approx 1/\sqrt{2}$.

Now, however, if we want to attach a particular *particle* to a particular lattice site we must write $\psi_{\uparrow\downarrow}$ so that it vanishes for $\vec{r}$ near $-\vec{\Delta}$ and it is nonzero for $\vec{r}$ near $\vec{\Delta}$; i.e.,

$$\psi_{\uparrow\downarrow} = \left[A \sum_{L\in \mathrm{E}} R_L^+(r) Y_{L0}(\Omega) + B \sum_{L\in \mathrm{O}} R_L^-(r) Y_{L0}(\Omega)\right] \alpha(1)\beta(2), \tag{C10}$$

with $A \approx B \approx 1/\sqrt{2}$. From Eqs. (C2)–(C5) this requires

$$\psi_{\uparrow\downarrow} = \frac{1}{\sqrt{2}} \left[A \sum_{L\in \mathrm{E}} R_L^+(r) Y_{L0}(\Omega) + B \sum_{L\in \mathrm{O}} R_L^-(r) Y_{L0}(\Omega)\right] X_{00}$$

$$+ \frac{1}{\sqrt{2}} \left[A \sum_{L\in \mathrm{E}} R_L^+(r) Y_{L0}(\Omega) + B \sum_{L\in \mathrm{O}} R_L^-(r) Y_{L0}(\Omega)\right] X_{00} . \tag{C11}$$

Thus unphysical wave functions (not properly antisymmetrized) are introduced into the problem.

A calculation of the pair wave function with a biased single-particle potential forces the wave function away from $-\vec{\Delta}$ and toward $\vec{\Delta}$. A definite constraint on the sharing of the wave function between the even and odd partial waves is introduced through the biased single-particle potential. Should the biased single-particle potential be removed there is no way in a two-particle calculation to prevent the pair wave function from condensing into a single energetically favorable state, e.g., $^1S_0$.

We have done our Hartree-Fock t-matrix calculation with a particular spin associated with a particular lattice site. Our wave functions are like Eq. (C1) with $A \approx B \approx 1/\sqrt{2}$. This constraint prevents the condensation of the wave function into the most energetically favorable state. It is not possible to prevent this condensation within an unconstrained two-body calculation.

APPENDIX D

In this appendix we consider the problem of evaluating the average value of $|D_0|^2$ and $(|D_1|^2 + |D_{-1}|^2)$ over the particles of the various shells of a bcc crystal (see Appendix A), where

$$|D_0|^2 = |D_{\bar{m}_s 0}(\beta_{ij})|^2 = \begin{cases} \cos^2\beta_{ij} & \text{for } \bar{m}_s = 0, \\ \frac{1}{2}\sin^2\beta_{ij} & \text{for } \bar{m}_s = 1, \end{cases} \tag{D1}$$

and

$$|D_1|^2 + |D_{-1}|^2 = |D_{\bar{m}_s 1}(\beta_{ij})|^2 + |D_{\bar{m}_s -1}(\beta_{ij})|^2 = \begin{cases} \sin^2\beta_{ij} & \text{for } \bar{m}_s = 0, \\ \frac{1}{2}(1 + \cos^2\beta_{ij}) & \text{for } \bar{m}_s = 1 . \end{cases} \tag{D2}$$

Let us recall that β_{ij} represents the angle between some externally chosen direction for the spin quantization axis and the direction of $\vec{\Delta}_{ij}$, which points from particle i to particle j. In particular, we wish to show that

$$\langle |D_0|^2 \rangle_{\text{shell}} = \tfrac{1}{3} \tag{D3}$$

and

$$\langle |D_1|^2 + |D_{-1}|^2 \rangle_{\text{shell}} = \tfrac{2}{3}, \tag{D4}$$

where $\langle\cdots\rangle_{\text{shell}}$ represents an averaging over the particles in any shell of a bcc lattice. This is equivalent to the vanishing of the quadrupole moment of particle density for each shell. That is, we must show that

$$\frac{1}{A}\sum_{j=1}^{A}[3\cos^2(\beta_{ij})-1]=0, \tag{D5}$$

where A represents the number of particles in a given shell surrounding particle i. If this is true, then Eqs. (D3) and (D4) are valid for both $\bar{m}_s=0$ and 1. The vanishing of the quadrupole moment of particle density is guaranteed by the cubic symmetry of the bcc lattice. Equations (D3) and (D4) thus are valid for all shells in a bcc lattice. We use this result in Appendix A to show that the contributions of a given shell towards the computation of $\bar{U}$ and U_0 in the Hartree-Fock t-matrix approximation can be replaced by an angular average over a uniform particle distribution.

---

*This work was supported in part by the National Science Foundation.

[1]G. Börner, in *Springer Tracts in Modern Physics*, edited by G. Höhler (Springer, New York, 1973), Vol. 69; V. Canuto, in proceedings of lectures given at NORDITA 1973–1974.

[2]D. Pines, J. Shaham, and M. Ruderman, Nat. Phys. Sci. 237, 83 (1972).

[3]P. W. Anderson and R. G. Palmer, Nat. Phys. Sci. 231, 145 (1971); J. W. Clark and N. C. Chao, *ibid.* 236, 37 (1972).

[4]D. Schiff, Nat. Phys. Sci. 243, 130 (1973).

[5]L. H. Nosanow and L. Parish, Ann. N. Y. Acad. Sci. 224, 226 (1973); V. R. Pandharipande, Nucl. Phys. A217, 1 (1973).

[6]E. Østgaard, Phys. Lett. 47B, 303 (1973).

[7]V. Canuto and S. M. Chitre, Phys. Rev. D 9, 1587 (1974); Phys. Rev. Lett. 30, 999 (1973).

[8]The t-matrix formulation of the quantum solid problem contains a self-consistent condition that can fail to be fulfilled. The satisfaction of the self-consistent condition is a necessary but not sufficient condition for a stable solid state.

[9]V. Canuto, S. M. Chitre, and J. Lodenquai (CCL), Nucl. Phys. A233, 521 (1974).

[10]S. Chakravarty, M. D. Miller, and C. W. Woo (CMW), Nucl. Phys. A220, 233 (1974).

[11]L. Shen and C. W. Woo, Phys. Rev. D 10, 371 (1974).

[12]R. A. Guyer, in *Solid State Physics*, edited by H. Ehrenreich, F. Seitz, and D. Turnbull (Academic Press, New York, 1969), Vol. 23, p. 413.

[13]R. V. Reid, Ann. Phys. (N.Y.) 50, 411 (1968).

[14]By the phrase "full solid-neutron-matter problem," we refer to the neutron solid problem with the complete set of state-dependent Reid soft-core potentials. For $L\geq 3$ we used the same approximation as Canuto and Chitre:

$$v(^1D_2) \text{ for even } L \text{ and } V_c(^3P_2-{}^3F_2) \text{ for odd } L.$$

[15]F. Iwamoto and H. Namaizawa, Prog. Theor. Phys. Suppl. 37, 243 (1966); B. Sarkissian, Duke Univ., thesis, 1969 (unpublished); R. A. Guyer and L. I. Zane, Phys. Rev. 188, 445 (1969); B. Brandow, Ann. Phys. (N.Y.) 74, 112 (1972); C. Ebner and C. C. Sung, Phys. Rev. A 4, 269 (1971); E. Østgaard, J. Low Temp. Phys. 5, 237 (1971). There are corrections to the simple formulas we use due to nonorthogonality, exchange, etc. Such corrections are discussed in the literature above that provides the background for the calculations we are carrying out. However, it is our view that if a solid state is to result, it will in fact occur at values of the parameters, e.g., $\alpha^2\Delta^2$, for which such corrections are small. We are guided in this belief by the results on solid ^{3}He.

Our H-F (Hartree-Fock) liquid energy, "half the Hartree liquid energy," is simply half of the Hartree potential energy. This is the correct energy to compare our calculations with: (1) By taking $\alpha^2\to 0$ we are assuming no kinetic energy; (2) at a density where the interparticle spacing is large compared to the range of the interaction the statistical correlations simply keep half of the particles away from a particular particle. Our H-F liquid energy is by no means the correct H-F liquid energy. But, it is the energy to which our calculation goes as $\alpha^2\to 0$; i.e., in the liquid limit of our calculation. We discuss our H-F liquid energy only in this context; it is a useful check on our numerical work.

We have carried our calculations to small α^2 ($\alpha^2 \leq \alpha_c{}^2$), not because we believe they are valid in this region, but because the literature contains a number of solutions to the homework problem in this particular region which we want to make comparisons with (e.g., CCL and CMW, Refs. 9 and 10, respectively). CCL and CMW do not account for nonorthogonality, etc. in their calculations. We would not be able to compare our results to theirs if we were to do a better calculation in the unphysical region.

[16]We use the result from bcc ^{3}He; this system is believed to be an antiferromagnet; S. B. Trickey, W. P. Kirk, and E. D. Adams, Rev. Mod. Phys. 44, 668 (1972).

[17]An analytic demonstration of the relationship of a variational calculation and the self-consistency condition is contained in Ref. 12 for the case of an α^2-independent t matrix. As the t matrix is only mildly α^2-dependent in the physical region this relationship "explains" the coincidence of $\alpha_{SC}{}^2$ and the α^2 at which the single-particle energy is a minimum.

[18]Østgaard, using a formalism quite similar to the one we employ, finds no satisfactory solutions in the physical region for a reasonable approximate pair interaction. See Ref. 6.

[19]The agreement between these calculations is that the self-consistent α^2 is small or unphysical.